Nanoscale Advances

ROYAL SOCIETY OF CHEMISTRY

REVIEW

View Article Online
View Journal | View Issue

Cite this: *Nanoscale Adv.*, 2021, **3**, 5745

Tuneable chemistry at the interface and self-healing towards improving structural properties of carbon fiber laminates: a critical review

Poulami Banerjee, Rishi Raj, S. Kumar* and Suryasarathi Bose *

Carbon fiber reinforced epoxy (CFRE) laminates have become a significant component in aircraft industries over the years due to their superior mechanical and highly tunable properties. However, the interfacial area between the fibers and the matrix continues to pose a significant challenge in debonding and delamination, leading to significant failures in such components. Therefore, since the advent of such laminated structures, researchers have worked on several interfacial modifications to better the mechanical properties and enhance such laminated systems' service life. These methods have primarily consisted of fiber sizing or matrix modifications, while effective fiber surface treatment has utilized the concept of surface energy to form an effective matrix locking mechanism. In recent times, with the advent of self-healing technology, research is being directed towards novel methods of self-healing interfacial modifications, which is a promising arena. In this review, we have provided comprehensive insight into the significance, historical advances, and latest developments of the interface of CFRE laminates. We have analysed the significant research work undertaken in recent years, which has shown a considerable shift in engineering the interface for mechanical property enhancement. Keeping in view the latest developments in self-healing technology, we have discussed reversible interfacial modifications and their impact on future improvements to service life.

Received 21st April 2021
Accepted 10th August 2021

DOI: 10.1039/d1na00294e

rsc.li/nanoscale-advances

1. Introduction

Carbon fiber-reinforced polymer (CFRP) composites were introduced in 1950, and by the 1980s, they found their way as a major component in structural applications. Defense-related aerospace industries and sporting goods are the major industries where CFRP composites are utilized to the greatest extent. In all these applications, epoxy has been the most commonly used polymer material followed by polyester, polyimide, polysulfone, vinyl ester, and other thermoplastic polymers.[1–3] The role of carbon fiber reinforced epoxy (CFRE) composites has been pivotal in shaping aircraft wings, fuselage, and other components due to their excellent and tunable mechanical properties, reduced weight, and thermal stability as well as galvanic corrosion resistance. Furthermore, carbon-based composites can provide electromagnetic induction (EMI) shielding against lightning strikes.[4–6] In such composites, carbon fiber (CF) reinforcements are the major load-bearing components, while the epoxy matrix acts as the base and the load transferring medium.

The interface plays a major role in determining the properties of CFRE laminates. The specific surface area that can reach up to 3000 cm^2 cm^{-3} for a considerable fiber volume fraction is quite high to provide enhanced interfacial area. CF's chemical inertness makes it difficult for a polymer to wet through it and develop a strong bond easily. An excellent adhesive property between the matrix and fibers constitutes a strong interface. The primary way to improve interfacial properties is to create a rough fiber surface through oxidation and etching. The increase in roughness increases interfacial area, thereby increasing interfacial strength. The other method of increasing interfacial strength is introducing surface functional groups that increase the affinity of the epoxy matrix for CFs through polar interactions.[7–12] Several researchers have worked on analysing the failure of fiber-based polymeric composites through interfacial micromechanical approaches[13–16] and spectroscopic characterisation of interfaces.[17].

The surfaces of polyacrylonitrile (PAN)-based CFs are non-homogeneous and have a skin–core structure. The graphitic basal planes at the skin are more aligned than those in the core. The presence of a disordered structure at the skin makes it very weak in shear. Moreover, the high degree of orientation in the skin region makes it more inert to react with the epoxy matrix and form a physical bond. Therefore, most manufacturers treat CFs with certain surface treatments, preferably sizing, to increase their compatibility with resins. These commonly include improving their compatibility with agents such as polyimide, epoxy, and polyvinyl alcohol through chemical reactions and incorporation of functional groups.[18] The surface

Department of Materials Engineering, Indian Institute of Science, Bangalore – 560012, India. E-mail: sbose@iisc.ac.in; skumar@iisc.ac.in

treatment of CFs for enhanced tensile properties was started as early as the 1970s, which did not yield many beneficial results. This was due to the associated fiber damage. Over a period of time, the interface has been modified by sustainable fiber surface treatments such as sizing, nanoparticle growth and deposition, matrix modification, and in some cases, a chemical/physical bond formation between the two components.[19] Since the interface between a continuous fiber and a resin extends along a larger area, it can essentially be treated as a third layer and termed 'interphase'.[8]

Of late, the concept of self-healing in aerospace components is being researched. These materials have the potential to substantially recover their load-transferring ability after damage.[20–23] Since the interphase is one of the pivotal components of a CFRP composite because of the gradient in properties in that region and a mismatch of thermal expansion coefficients, one of the major modes of failure of such composites is through delamination. Therefore, along with improvement in interfacial strength and toughness, recovery of the interface through both intrinsic and extrinsic mechanisms is being widely researched. White *et al.*[24] were the pioneers in the field of self-healing in polymeric composites by using a biomimetic method of micro-capsules triggered by an external stimulus such as heat, light, or moisture. An ideal self-healing material is expected to restore the original properties, making it safer and more durable for application purposes. These properties can include interfacial strength, flexural strength, tensile strength, stiffness, fracture toughness, fatigue strength, barrier properties, or even molecular weight. The method has been extended to the formation of thermo-reversible bonds between CFs and epoxy thereby restoring delaminated regions.[25]

In this review paper, we extensively discuss the structural properties of CFRE composites with the major focus on interfacial improvement. We have classified interfacial modification in terms of the protocols followed. We further discuss the fairly novel area of self-healing. To the best of our knowledge, this is the only article that provides an extensive study on the theory and methodologies of interfacial tuning of CF/epoxy composites, particularly those of laminated composites, encompassing a survey of about 50 years along with a detailed analysis of several state-of-the-art domains, with an additional section discussing the advancements in self-healing techniques in such composites in recent years.

2. Tailoring the interface

2.1. Sizing of carbon fibers

Sizing was a technique developed as early as the 1980s to protect the fiber surface from wrinkles or damage during manufacturing. An optimum sizing agent contains wetting properties to enhance the adhesion with the matrix as well.[26] However, it has not been as beneficial for CF systems as for glass fiber systems. Currently, three types of sizing agents are commercially used: (1) a sizing agent coated with an organic solvent, (2) an emulsified sizing agent dispersed in water, and (3) a water-soluble sizing agent.[27,28]

Traditionally, epoxy dissolved in some organic solvents served as the sizing agent for CFRE composites. Once the sizing is done, the solvent is evaporated by heating the fibers in a chamber at a temperature higher than the solvent's boiling point.[29,30]

One of the earliest attempts to analyze the effects of sizing and surface treatment on carbon CFs was made by Harris *et al.*[31] They treated the fibers with dip coating, electro-polymerization, and plasma polymerization, and thereafter, compared the dynamic mechanical properties. The aim was to thinly coat a polymeric layer rich in nitrogen-containing groups to increase the compatibility with the amine-cured epoxy matrix. It was observed by DMTA that parameters such as the loss peak temperature, T_a (and the related power-law characteristic temperature, T_o), the peak height (tan δ) (and the related power-law A parameter), and the power-law exponent n, which relates to the shape of the lower-temperature wing of the loss peak, experienced a shift.

On analysis of the shift in viscoelastic properties as fitted in the Debye's function,

$$\tan\delta = \frac{A}{[\omega\tau_o(1 - T_o/T)^{-\alpha}]^{-m} + [\omega\tau_o(1 - T_o/T)^{-\alpha}]^{1-n}} \quad (1)$$

it was observed that both T_a and T_o experience a slight decrease with oxidation, electro-polymerization and plasma polymerization treatments, and a slight increase with thicker dip-coatings. A similar fall was indicated for A (peak height) following the treatments which increased the IFSS τ_i, while n (indicating a downward displacement of the left-hand wing of the peak) rose somewhat erratically with increasing τ_i. These observations relate to the oxidation, electro-polymerization and plasma polymerization treatments only, because no shear strength measurements were made for the dip coatings. An increase in n and a fall in T_o are both associated with lowering of the peak temperature, but occur together, without a simultaneous change in 'm'. They suggest an associated slight broadening of the peak and a modest reduction in thermal stability. Only the composite with thicker latex dip-coated fibers showed a clear indication of a raised loss peak temperature, indicating a difference in character between this interphase and the type of interphase/interface present in composites representing all other surface treatments. They finally concluded based on a contradictory result from previous research that the enhancement in interfacial strength was not directly related to any corresponding shift in the viscoelastic properties as measured by DMTA.

The possible limitations of a sizing agent in certain cases were presented by Park *et al.*[32] Eight plies of CFs were impregnated with phenolic resin to fabricate a laminate. Two such laminates were prepared, one with the sizing agent and one without. The fiber volume fraction was maintained at 60 vol%. Thermo-mechanical analysis indicated a lower thermal expansion in the case of unsized CFs in comparison to the sized ones. This was attributed to the poor adhesion of the sizing agent and its outgassing during the carbonization process. Acoustic emission tests revealed fiber–matrix debonding to be the major cause of failure for the sized fiber composites, indicating that

sizing reduced the fibers' ductility and crack absorbing potential. Thus, their work effectively showed the importance of a suitable sizing agent for better mechanical properties.

Dai *et al.*[33] studied the comparative effects of sizing on the IFSS of CFRE composites by subjecting two types of fibers, namely, CF T300B (carbon fiber mat) and T700SC (short carbon fibers) to de-sizing in acetone at 75 °C for 6 hours. The interfacial strength of the resulting composites was assessed using a microdroplet test. It was observed that the dispersive component of the surface free energy increased after de-sizing for both T300B and T700SC. At the same time, the polar components of the surface free energy in both fiber types decreased after de-sizing, indicating a decrease in the percentage of epoxide, hydroxyl, and ether groups. Furthermore, the IFSS increased on desizing, which was attributed to the enhanced dispersive surface energy and the fact that sizing turned the fibers brittle. It was also concluded that the presence of a thick sizing layer decreased the interaction of the CFs with the epoxy matrix. Improvement in the interfacial properties and the corresponding changes in the fiber surface due to functionalization are shown in Fig. 1.

Eyckens *et al.*[34] studied the effects of different kinds of sizing agents on CFs and their effects on the improvement of fiber to matrix adhesion. The synthesis of two different types of ionic liquids (ILs) was done for 'sizing'. Since imidazolium-based ILs are known to enhance plasticity in polymers, BmimCl was used as one of the sizing agents. The other was from a relatively new class of ILs known as solvate ionic liquids (SILs). Sizing baths were prepared with 10% wt/vol solution of the IL in deionized water. Fiber tows were dipped in the sizing bath for 10 min followed by drying. Single fiber pull-out tests were conducted against maleic anhydride grafted polypropylene (MAH-*g*-PP). The addition of BmimCl to unfunctionalized (UF) fibers gave an increase in adhesion of 66% (from 15.4 ± 1.9 MPa for UF US to 25.5 ± 1.8 MPa for UF BmimCl). However, BmimCl proved to be incompatible with the matrix resin. In the single fiber fragmentation test, it was observed that coating the fiber surface with BmmiCl and G_3TFSA (the new class of sizing agents) increased the interfacial strength up to 106% (37 ± 4.1 MPa) and 53% (27 ± 3.4 MPa), respectively, from the 18 ± 1.1 MPa of the unsized fibers. The purpose of the introduced ILs was to act as a plasticizer and effectively dissipate the energy while undergoing a shear deformation. The molecular structure of the ILs and their grafting techniques with subsequent improvement in the interfacial properties are shown in Fig. 2.

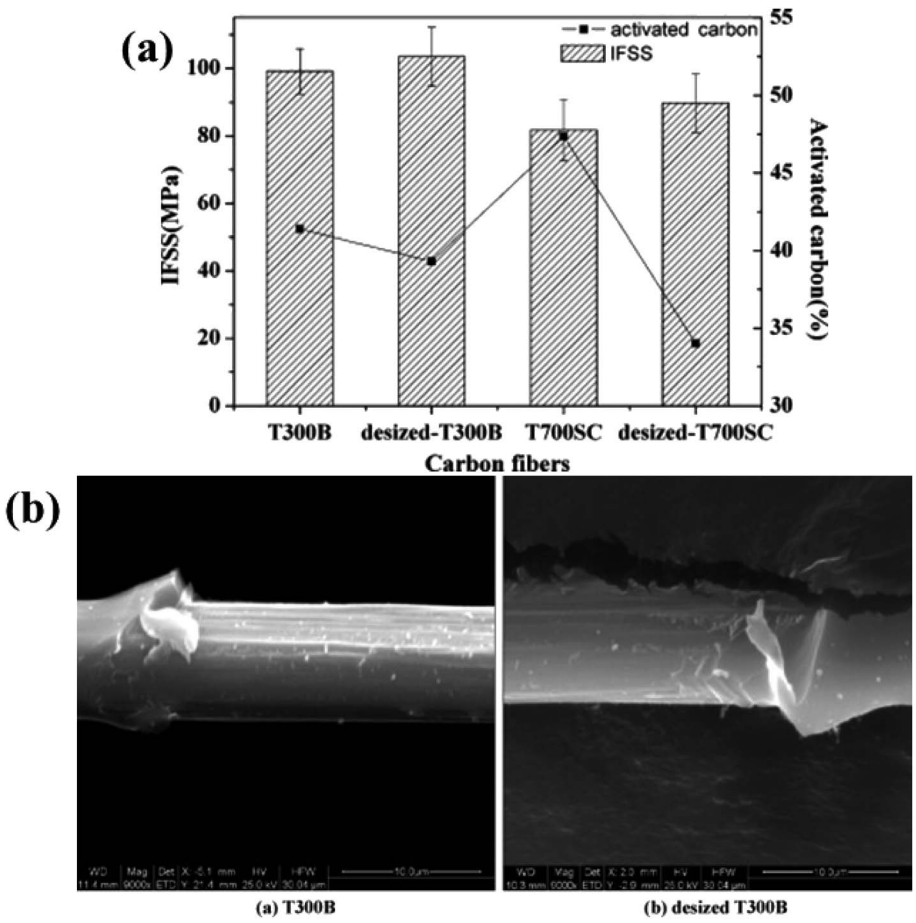

Fig. 1 (a) Bar diagram representing the change in IFSS on desizing of carbon fibers and (b) SEM micrograph showing the increased surface roughness post desizing.[33] Reproduced from ref. 33 with permission from Elsevier (2011).

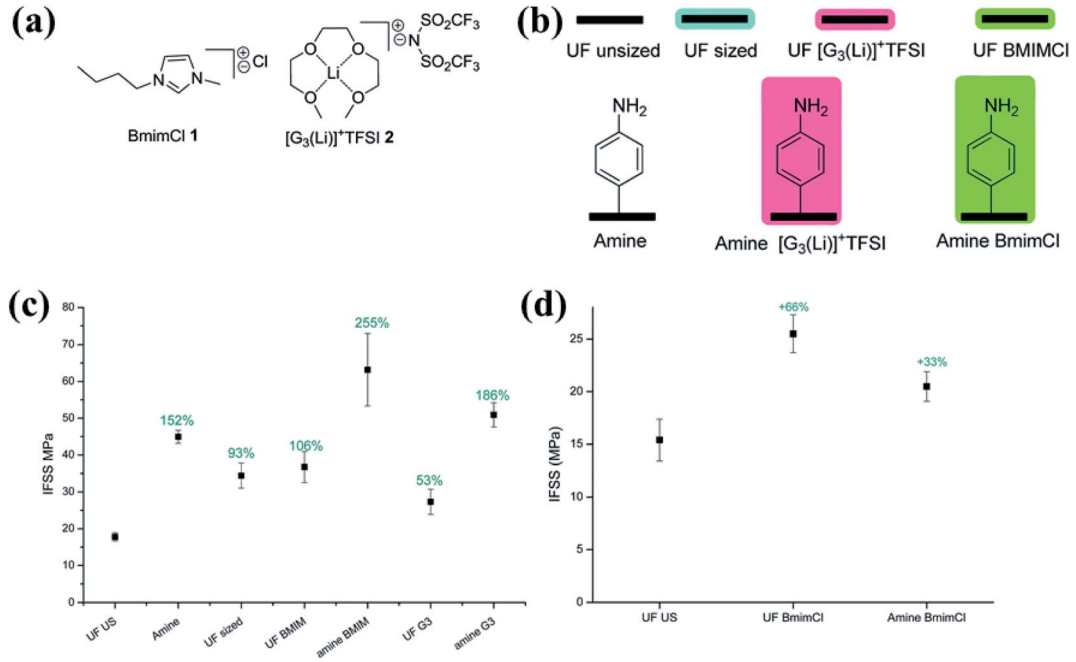

Fig. 2 (a) Molecular structure of the two ILs. (b) Grafting of the ILs over carbon fibers with color codes. (c) IFSS strength of control and treated fibers in epoxy resin (percentage increases are relative to that of the unfunctionalized, unsized fiber (UFUS) sample shown in teal). (d) IFSS of functionalised fibers in MAH-*g*-PP *via* fiber pull-out (percentage increases in IFFS are relative to that of the UFUS fiber sample shown in teal).[34] Reproduced from ref. 34 with permission from RSC (2018).

Yuan *et al.*[35] developed a polyacrylate emulsion sizing and coated it over unsized unidirectional (UD) fibers, followed by fabrication of laminates in a mold. This was followed by curing to solidify the specimens. The resin content in the sizing agent was maintained at 30–40%. Virgin CF-based laminates were also prepared by the same method as control samples. It was observed that the ILSS of the synthesized sizing-based laminates increased from 81.2 MPa to 92.7 MPa, *i.e.*, by 14.2%. This was higher than that of the laminates with commercial sizing (86.7 MPa) indicating that the laboratory-sized fibers were more compatible with the interface than the commercially sized ones because of better van der Waals interaction and functional incorporation.

Beggs *et al.*[36] performed surface functionalization of unsized CFs using diazonium salts. They functionalized CFs with aryl-diazonium salts and formed composites for IFSS measurements. Their work primarily focused on diluting the surface-functionalized reagents and did not hamper the IFSS, thereby allowing for surface grafting of a larger CF volume. At a concentration of 50% of salts, the fibers were shown to give optimum IFSS results. They inferred that it was possible to double the amount of fibers with the original amount of raw materials without causing any deterioration in the interfacial properties.

One critical takeaway from the advancement in the research on sizing agents is their importance, both in terms of their ratio with respect to the fibers and their chemical nature for the improvement of the interfacial properties of composites. However, while most manufacturers restrict from providing the background information on the chemical mixture of their

Table 1 Mechanical property improvement for various sizings in carbon fiber–epoxy composites

Sl no.	Protocol	Mechanical property	Improvement over the control sample	Ref.
1	Dip coating, electropolymerisation, plasma polymerisation	Viscoelasticity	No correlation	31
2	Phenolic resin	Flexural strength	Decrease	32
3	Removal of commercial sizing agent	IFSS (microdroplet test)	38% (T300B) 9% (T700SC)	33
4	Sizing with (1) BmmiCl (2) G_3TFSA	IFSS (SFFT)	106% 53%	34
5	Polyacrylate emulsion sizing	ILSS	14.2%	35
6	Diazonium salt sizing	IFSS (SFFT)	40 ± 7% (for 50% treatment)	36

commercial sizing agents, new sizing development continues to be carried out by a very small number of researchers in carbon fiber manufacturing laboratories. Consequently, it appears likely that the nature of all the interactions involved in size formulations, size application, fiber drying, fiber wetting impregnation and composite performance is not fully understood, even by those with inside knowledge of size formulations, indicating a serious barrier to the innovation of better CFRE materials and is something that needs to be addressed on an industrial level.

A summary of the above results is presented in Table 1.

2.2. Modification of the epoxy matrix

One of the earliest studies in understanding the interfacial reactions of carbonaceous modifications of the epoxy matrix with CFs was conducted by Andrew Garton and his team in 1987.[37] They modified the epoxy matrix with carbon black, crushed CFs, and chopped CFs, respectively. A part of the carbon black was air-oxidized, and another part was nitric acid oxidized. It was observed that initially the presence of carbon black increased the rate of consumption of the epoxide groups and at a later stage, it was inhibited. The residual epoxide amounts at the end of the cure were higher in the presence of carbon black than what it was in its absence. The same effect was observed in the crushed CF case, while the chopped CFs showed no effect over the cure kinetics. This was explained by the oxidized carbon surface acting as a catalyst for epoxy–primary amine cure reactions. However, the start of epoxy–secondary amine cure reactions was inhibited by steric hindrance of the adsorbed material on the carbon surface.

Following the same line of protocol, researchers modified the epoxy matrix to ascertain its influence on the interfacial properties over the years. Xu *et al.*[38] modified epoxy with clay using a hot-melt method. They fabricated laminates using the hand-layup and vacuum bagging method. The amount of clay was varied at 0 phr, 2 phr, and 4 phr, and a fiber volume fraction of 65.1%, 61.9%, and 60% was, respectively, attained. Mode I interlaminar fracture toughness, G_{IC}, increased by 53% and 85% with the increase in clay percentage. SEM images of the fracture surfaces revealed that while the CF surfaces with neat epoxy appeared smooth, those with modified epoxy had bits of resin adhered to their surface, thus indicating better adhesion and wettability of the modified matrix. Flexural strength too showed an increase for 2 phr clay modified epoxy laminates but decreased for laminates with 4 phr clay modified epoxy. This was attributed to the agglomeration of clay nanoparticles at the larger concentration. In another study using similar components, Oliwa *et al.*[39] modified an epoxy matrix with various percentages of bentonite clay (0, 1 and 3 wt%) to determine the influence of organoclay (bentonite BS) modified with quaternary ammonia (QAS) and phosphonium salts (QPS) on the mechanical properties of the CF-modified epoxy laminates. While a decrease in tensile strength was observed, Young's modulus was increased in the 0° fiber direction with an increase in the percentage of clay. This was attributed to the increase in the resulting fibers' brittle behavior which decreased the strength, while the increase in stiffness of the resulting fibers led to an increase in Young's modulus. The ILSS experienced a slight decrease with the clay addition. This was attributed to the orientation of the organoclay platelets which did not hinder the direction of crack propagation and provided no resistance to delamination. Flexural strength of the composites containing 1 wt% BSQAS and BSQPS improved by 4% and 10%, respectively.

The recent methods for modifying epoxy composites for better interfacial properties include modifying them with carbonaceous nanoparticles, particularly graphene-based derivatives and carbon nanotubes (CNTs).[40–46] Both these nanoparticles are usually surface functionalized for better compatibility with the epoxy matrix. Pathak *et al.*[47] prepared CF–epoxy laminates by adding 0–0.6 wt% graphene oxide (GO) in the epoxy. The flexural strength increased by 40% and ILSS increased by 23% up to 0.3 wt% GO and then decreased with further increase in GO content. The O–H groups of CFs attack the carbon of GO in epoxy, which results in the opening of a strained ring thus forming an ether bond which increases the affinity of GO for CFs. GO also contains oxygen function groups on its surface and edge increasing the CF surface's polarity, which leads to the effective bonding between GO and the matrix thereby improving its mechanical properties. Furthermore, with an increase in GO content, GO reacts with the amine hardener (TETA molecules), leaving fewer TETA molecules to react with epoxy, thereby decreasing the degree of cross-linking. This has been directly correlated to the loss of ILSS values beyond an optimum percentage of GO in the epoxy.

Chiou *et al.*[48] worked on graphene nano-platelets (GNPs) functionalized with maleic anhydride and nano-carbon aerogels (NCA) functionalized with amines to form a GNP/NCP/epoxy hybrid matrix *via* ultrasonication to disperse the nanoparticles well into the resin. Next, CFRE laminates were fabricated using a fixed mixing ratio (5 : 5) and by adding four different proportions of GNP/NCA hybrids (*i.e.*, 0.25, 0.5, 0.75 and 1.0 wt%). It was observed that the mechanical properties, *viz.*, tensile, flexural and impact strength, of the laminates containing 1 wt% of the GNP/NCA hybrids were superior to those of the laminates containing 1 wt% of a single carbon nanomaterial. However, an increase in the content of the CAs reduced the flexural modulus of the laminates owing to them being a 'soft' reinforcement, thereby lowering the stiffness of the laminates. The impact strengths of the CFRE laminates fabricated with 0.25 wt% and 0.5 wt% hybrids were improved by 9.3% and 10.2%, respectively. The GNP/NCA hybrids also resulted in an increase in fatigue life cycles. The major mechanism for the improvement of strength and toughness in the laminates was crack pinning and crack deflection. While the soft NCAs effectively absorbed the energy of cracks and arrested their propagation, GNPs assisted in crack deflection. This helped increase the strength, fracture toughness, impact toughness, and fatigue life of the laminates. Fig. 3 indicates the entire process of formation of the CF/epoxy nanocomposites and the CFRE hybrid laminates.

In the next line of carbonaceous materials, CNT-modified epoxy matrices and their effect on the interfacial properties of

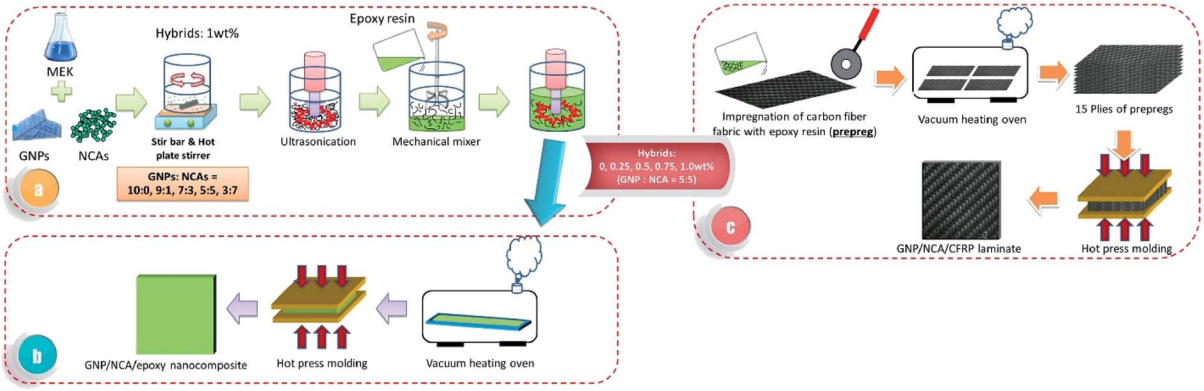

Fig. 3 Preparation of the carbon hybrid/nano-composites and CFRE laminates.[48] Reproduced from ref. 48 with permission from Elsevier (2019).

CFRE laminates have also been widely investigated. Kim *et al.*[49] presented their work on acid and amine-functionalized CNTs. Functionalized CNTs were dispersed in epoxy *via* ultrasonication and impregnated onto CFs to form the laminates. In all these laminates, the functionalized CNT percentage was kept at 2 wt%. It was observed that the silane-modified laminates exhibited flexural modulus and flexural strength higher than the neat CFRE laminates and acid-functionalized CNT-CFRE laminates by 11% & 55%, and 5% & 15%, respectively. Improved dispersibility and better interfacial interaction were attributed to the better mechanical properties.

In another study, Chou *et al.*[50] functionalized MWCNTs with 4,4-methylene diphenyl isocyanate (MDI) in a reflux condenser under a N_2 atmosphere. The matrix was a blend of epoxy (EP, 60 wt%) and polybenzoxazine (PBZ, 40 wt%). Modified nanocomposites were prepared by dispersing different concentrations of modified CNTs (0.25, 0.5, and 0.75 wt%) in the EP/PBZ matrix in a butanone solvent followed by curing and post-curing. CFRE laminates were prepared by impregnating the modified matrix into each mat individually, placing them in a hot air circulating oven and then subjecting to hot compression molding. The increase in ILSS, flexural, torque, impact, and tensile strengths for the 0.5 wt% CNT modified laminates was the highest, 24.6%, 6.9%, 6.5%, 5.5%, and 1.7%, respectively, in comparison to the neat laminates. Delamination was observed to be the major mode of failure in the modified CFRE laminates.

Quan *et al.*[51] studied the influence of CNTs on the fracture toughness of CFRE laminates. They observed an increase in the average mode II fracture toughness by 68% and 171% with the addition of 0.5 and 1 wt% CNTs, respectively. This was attributed to the extremely good mechanical interlocking of the interface and crack deflection with the addition of CNTs.

Not much research has been conducted on modifying epoxy resin with metal oxide particles for improvement in mechanical properties. Earlier work by Hussain *et al.*[52] involved modifying the epoxy matrix with 10 vol% of micro and nano-sized Al_2O_3 particles *via* filament winding to create hybrid CFRP (HCFRP) composites. An increase in fiber volume fraction increased the ILSS of both neat CFRE laminates and micron-sized HCFRP composites. It was observed that the addition of the fillers increased the interfacial strength, thereby improving the ILSS. However, for nanosized HCFRP composites, the ILSS increased up to 35 vol% of fibers after which it started decreasing. A decrease in ILSS above this fraction of fiber content of nanosized HCFRP composites suggested crack propagation through the fiber–matrix interface. The number of particles was inversely proportional to the square of their diameters at a given volume percent. As the particle size decreases, the number of contact points increases substantially, resulting in higher mechanical interlocking and high friction coefficient. Furthermore, fracture toughness increased by 40% with the addition of nano- or micro-sized fillers. Crack deflection and crack blunting were the major mechanisms for the increase in fracture toughness.

Several hybridized laminates have been researched upon where more than one type of nanoparticles were dispersed in the epoxy matrix. Ulus *et al.*[53] modified the epoxy matrix with boron nitride nanoparticles (BNNPs) and CNTs. The VARTM process prepared the resulting laminates. BNNPs and CNTs were added at 0.5 wt% and 0.3 wt% to the epoxy resin. The shear strength values for neat epoxy/CF, CNT-epoxy/CF, BNNP epoxy/CF, and BNNP-CNT-epoxy/CF laminates were observed to be 30 $\pm$ 2.3 MPa, 40 $\pm$ 4.2 MPa, 54 $\pm$ 2.7 MPa, and 58 $\pm$ 3.6 MPa, respectively. Thus, the highest enhancement in strength and strain was obtained for BNNP-CNT modified laminates. SEM micrographs of the BNNP-CNT modified laminates showed wavy striations on the CF's surface compared to the smooth nature of the neat CF for the unmodified laminates. The wavy surfaces can be related to plastic deformation and energy consumption, which result in toughness increase of the epoxy matrix with nanoparticles. Furthermore, an increase in toughness of the epoxy matrix was observed because of the nanoparticles, which acted as crack energy absorbers and crack deflectors. At the same time, the CNT pull-out failure mode requires higher energy, which in turn increases the toughness of the laminates.

Bisht *et al.*[54] formed a 3D structure with graphene (Gr-sheets), nano-diamonds (ND-particles), and CNT-tubes. The homogeneously dispersed NDs were partly mixed with Gr

solution, and the other part with CNT solution. Both the thoroughly mixed solutions were mixed and ultrasonicated to form a final homogeneous solution. The hybrid solution was thoroughly dispersed over epoxy and the laminate was fabricated through vacuum bagging. Both interlaminar and intralaminar mode I fracture toughness revealed improvement of ~260% and ~53%, respectively, with 25Gr:50CNT:25ND CF/epoxy, compared to the neat CF/epoxy composite marking a total improvement of ~1523% over pure epoxy for intralaminar fracture toughness. An improvement of ~60% and ~16% in tensile strength and ILSS, respectively, was observed. Suitable dispersion of the nanofillers and improved adhesion between the matrix and the fibers were cited as the reasons. Along with an improvement in strength, strain too showed an improvement with the addition of nanoparticles. The rotation of the NDs because of their spherical morphology allowed the polymer chains to easily slide and dissipate energy thereby increasing the strain of the laminates. The high aspect ratio of the CNTs also allowed the crack to propagate to a larger distance before failure. Fracture toughness witnessed an increase because of the increase in both adhesion and crack-resisting ability of the hybrid laminates. The variation in the fractured surfaces of the

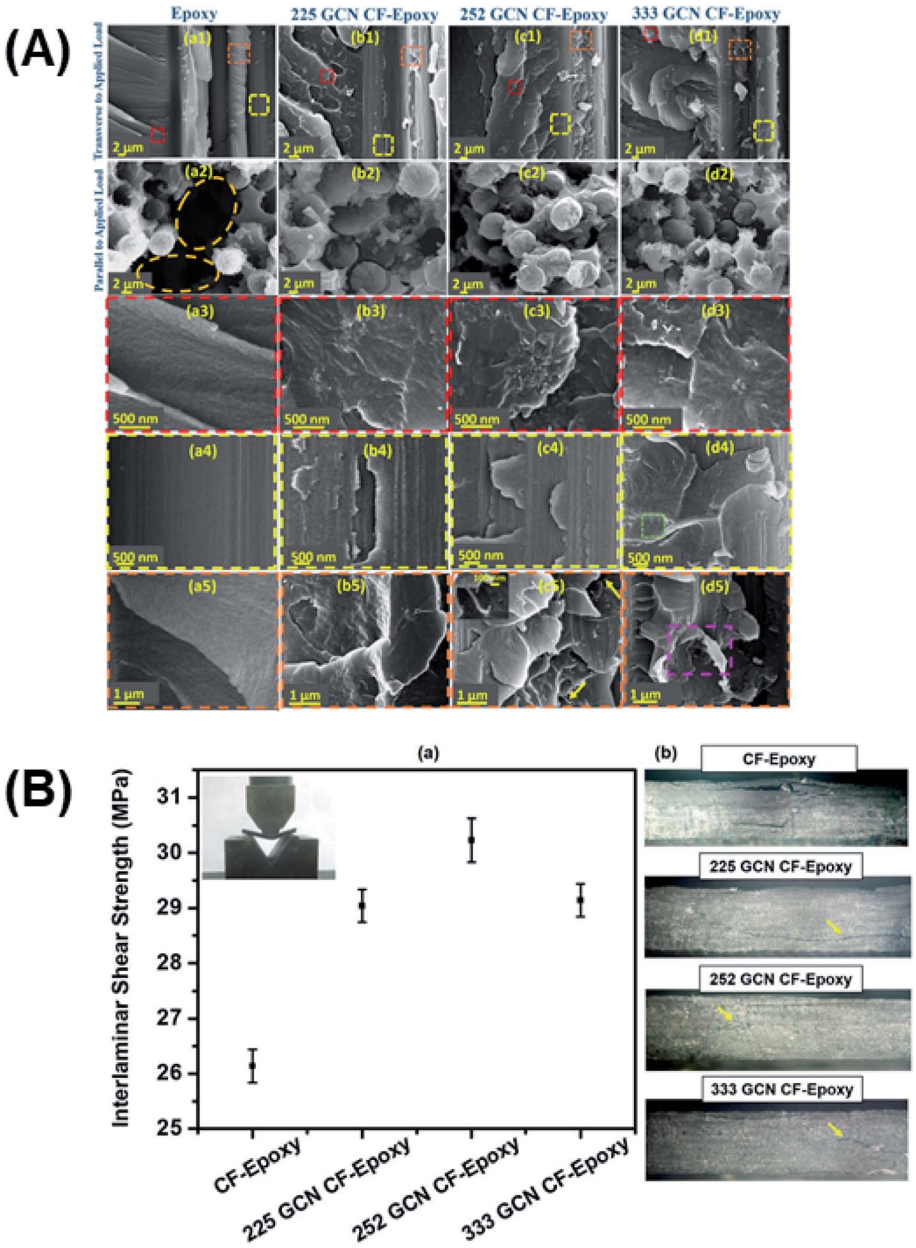

Fig. 4 (A) SEM images of the fractured surface cross-sections both along and transverse to the direction of the applied load for (a(1–5)) CF–epoxy, (b(1–5)) 25Gr:25CNT:50ND CF–epoxy, (c(1–5)) 25Gr:50CNT:25ND CF–epoxy and (d(1–5)) 33Gr:33CNT:33ND CF–epoxy composites at different magnifications. (B) ILSS plots for CF–epoxy and various combinations of the Gr:CNT:ND CF–epoxy composite.[54] Reproduced from ref. 54 with permission from Elsevier (2019).

reinforced laminates with varying percentages of the nanofillers and the improvements in their mechanical properties are shown in Fig. 4.

Katti *et al.*[55] worked on grafting hydroxylated poly(ether ether ketone) (HPEEK) over GO, which was then dispersed in epoxy resin. This modified epoxy matrix was infused into CFs *via* the VARTM technique. It was observed that the interface between the CFs and epoxy improved with the matrix modification. This improvement was reflected in an increase in tensile strength and ILSS by 9 and 11%, respectively. The nanoparticles' agglomeration was prevented through mechanical stirring and bath sonication of the HPEEK–GO suspension both before mixing and after mixing with epoxy. SEM fractographs shown in Fig. 5 confirmed better interfacial adhesion of the epoxy to the fibers because of GO "interconnects".

Thus, nanoparticles in epoxy resins have been shown to improve interfacial strength and restrict crack propagation in the matrix, thereby improving mechanical properties. While

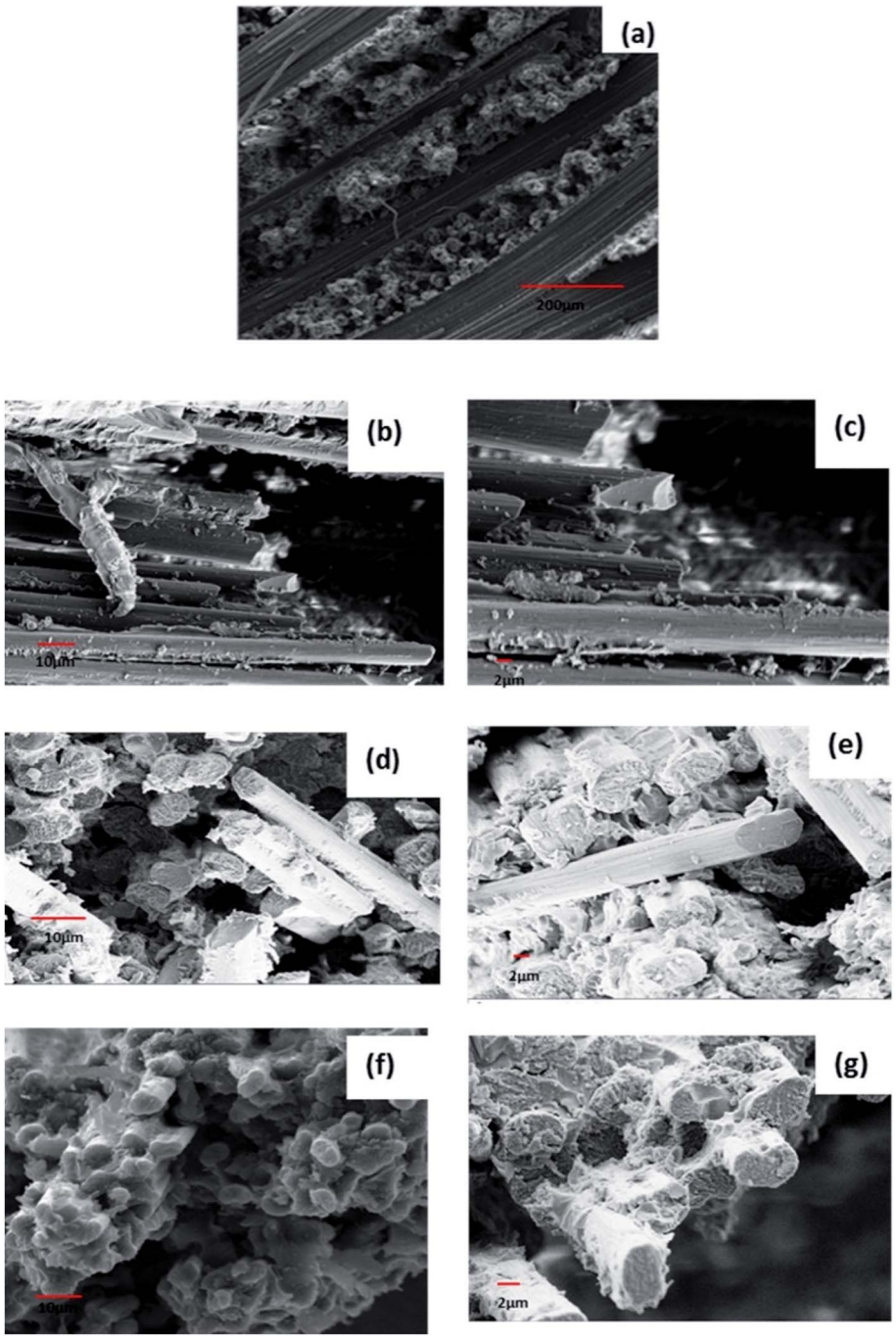

Fig. 5 Fractured SEM images of (a–c) epoxy/CF, (d and e) epoxy/CF laminates containing GO, and (f and g) epoxy/CF laminates containing HPEEK-*g*-GO.[55] Reproduced from ref. 55 with permission from Elsevier (2018).

Table 2 Mechanical property improvement for various matrix-modifications in carbon fiber–epoxy composites

Sl no.	Fillers	Types/concentrations	Mechanical properties	Improvement over control sample	Ref.
1	Clay	2 phr	Mode I fracture toughness	53%	38
		4 phr		85%	
2	Clay	BSQAS-1 wt%	Flexural strength	4%	39
		BSQPS-1 wt%		10%	
3	GO	0.3 wt%	ILSS	23%	47
4	GNP:NCA	0.25 wt%	Impact strength	9.3%	48
		0.5 wt%		10.2%	
5	Silane modified MWCNTs	2 wt%	Flexural strength	55%	49
			Flexural modulus	11%	
6	MDI modified MWCNTs	0.5 wt%	ILSS	24.6%	50
			Flexural strength	6.9%	
			Torque	6.5%	
			Impact strength	5.5%	
			Tensile strength	1.7%	
7	MWCNTs	0.5 wt%	Mode II fracture toughness	68.11%	51
		1 wt%		171.02%	
8	Al_2O_3	Nano-sized	ILSS	20%	52
		Micro-sized		43%	
		Both nano and micro-sized particles	In-plane strain fracture toughness	40%	
9	Gr:ND:CNT	25Gr:50CNT:25ND	Interlaminar mode I fracture toughness	260%	54
			Intralaminar mode I fracture toughness	53%	
			Tensile strength	60%	
			ILSS	16%	
10	HPEEK-grafted GO	0.5 wt%	Tensile strength	9%	55
			ILSS	11%	

carbonaceous particles emerged as some of the primary nanofillers owing to their high dispersibility, hybridization over the years has led to structures with better affinity towards adhesion on epoxy. Therefore, nanofiller modification has been one of the biggest developments in mechanical aspects of composite fabrication. Because of their ease of fabrication that entails only proper dispersion of fillers, nanofiller modified epoxy laminates continue to have wide application in aerospace, automotive, electronic goods, and sport-based industries.

A summary of the above results is presented in Table 2.

2.3. Modification of carbon fibers

2.3.1. Oxidative surface treatment. To improve the adhesion between the CFs and matrix, several surface treatments are performed on CFs. There are several methods of oxidative surface treatment, primary methods amongst them are dry oxidation in the presence of gases, plasma treatment, and wet oxidation.[56]

Dry oxidative treatments are normally performed with air, oxygen, and CO_2 at low or elevated temperatures. Herrick *et al.*[57] treated rayon-based CFs in air at 500 °C for 16 h to slightly improve the ILSS. The ILSS was improved by 45% when the temperature was raised to 600 °C, although a serious weight loss accompanied. Scola *et al.*[58] treated the fibers for 60 s in N_2 containing 0.1–1.8% O_2 at 1000–1500 °C to improve their bonding characteristics in a resin. There was no significant degradation of the mechanical properties of the fibers. Dai *et al.*[59] studied the effect of heat treatment on CF surface properties and fiber/epoxy interfacial adhesion. T300B CFs were heated in a vacuum drying chamber at 150 °C, 180 °C, and 200 °C for several hours using controlled processing cycles. It demonstrated that the content of activated carbon atoms (in conjunction with oxygen and nitrogen and hydroxyl) on the treated CF surface and the polar surface energy decreased with increasing the heat treatment temperature. Compared with the untreated fibers, the wettability studied by a dynamic contact angle test between CFs and E51 epoxy resin became worse. The results of micro-droplet tests demonstrated that the IFSS of T300B/epoxy reduced after the heat treatment process. This was attributed to the decrement of the amount of reactive functional groups in the interfacial region.

Plasma treatment has become a popular method for improving the fiber–matrix adhesion in recent years.[60–70] Plasma is a partially or fully ionized gas containing electrons, radicals, ions, and neutral atoms or molecules. The principle of plasma treatment is the formation of active species in a gas induced by a suitable energy transfer. Typical gases used to create plasma include air, oxygen, ammonia, nitrogen, and argon. Erden *et al.*[70] used continuous atmospheric plasma oxidation (APO) to introduce oxygen functionalities on the surface of CFs to improve the interfacial adhesion between CFs and polyamide-12 (PA-12). After the APO treatment, CFs became more hydrophilic due to the introduction of polar oxygen-containing groups on the fiber surface, which also increased fiber surface energy. The fiber tensile strength remained unaffected. The

IFSS between CFs and PA-12 increased from 40 to 83 MPa with up to 4 min of APO treatment. This can be attributed to the increase of surface oxygen content from 7 at% to 16 at%, which yielded more hydrogen bonds between the fibers and PA-12 matrix. Several liquid-phase oxidizing agents (*e.g.*, nitric acid, acidic potassium permanganate, acidic potassium dichromate, hydrogen peroxide, and ammonium bicarbonate) were also used to treat the CF surface. These liquid-phase treatments do not cause excessive pitting and the subsequent degradation of the fiber strength.[71]

Anodic oxidation is most widely used for the treatment of commercial CFs as it is fast, uniform and suited to mass production.[72,73] CFs act as an anode in a suitable electrolyte bath. A potential is applied to the fibers to liberate oxygen on the surface. Typical electrolytes include nitric acid, sulfuric acid, sodium chloride, potassium nitrate, sodium hydroxide, ammonium hydroxide, and so on.

Non-oxidative methods, including the deposition of an active form of carbon, plasma polymerization, and grafting of polymers onto the fiber surface,[74] were used for the CF surface treatments. Whiskerization involves the growth of thin and high strength single crystals, such as silicon carbide, silicon nitride, and titanium dioxide, at right angles to the fiber surface.[75] Many polymerizable organic vapours are used for the plasma polymerization process, such as polyamide, polyimide, organo-silanes, propylene, and styrene monomers. Plasma polymerization is demonstrated to increase the polar component of the surface free energy of CFs.[76,77]

Earlier studies on surface functionalization included the attempt by Pittman *et al.*[78] to quantify the amount of acid and amine functionalities on the surface of CFs. Acid and amine treatments were conducted on CFs with HNO_3 and tetraethylenepentamine (TEPA), respectively. The determination of acid functional groups was undertaken through a combination of NaOH uptake and methylene blue adsorption experiments. A certain amount of CFs was dipped in NaOH solution and the difference in concentration of NaOH, as determined from a pH meter, indicated the initial amount of acid functions on the CF surfaces. Next, a dye adsorption study was undertaken by adding 1 ml of 1 M NaOH solution to 11 ml of methylene blue (MB) solution to adjust the solution pH to about 10.8–11 to deprotonate the surface-active acid moieties. Then, the fiber specimen was immersed in 50–300 ml of MB solution for 16 h. A spectrophotometer calculated the absorbance of the MB solution and the difference in the dye concentration was used to calculate the surface acidic functional groups. The same protocol was used to determine the amount of basic functional groups over the CF surface. An initial acid uptake with HCl solution and a later metanil yellow anionic dye adsorption were used to

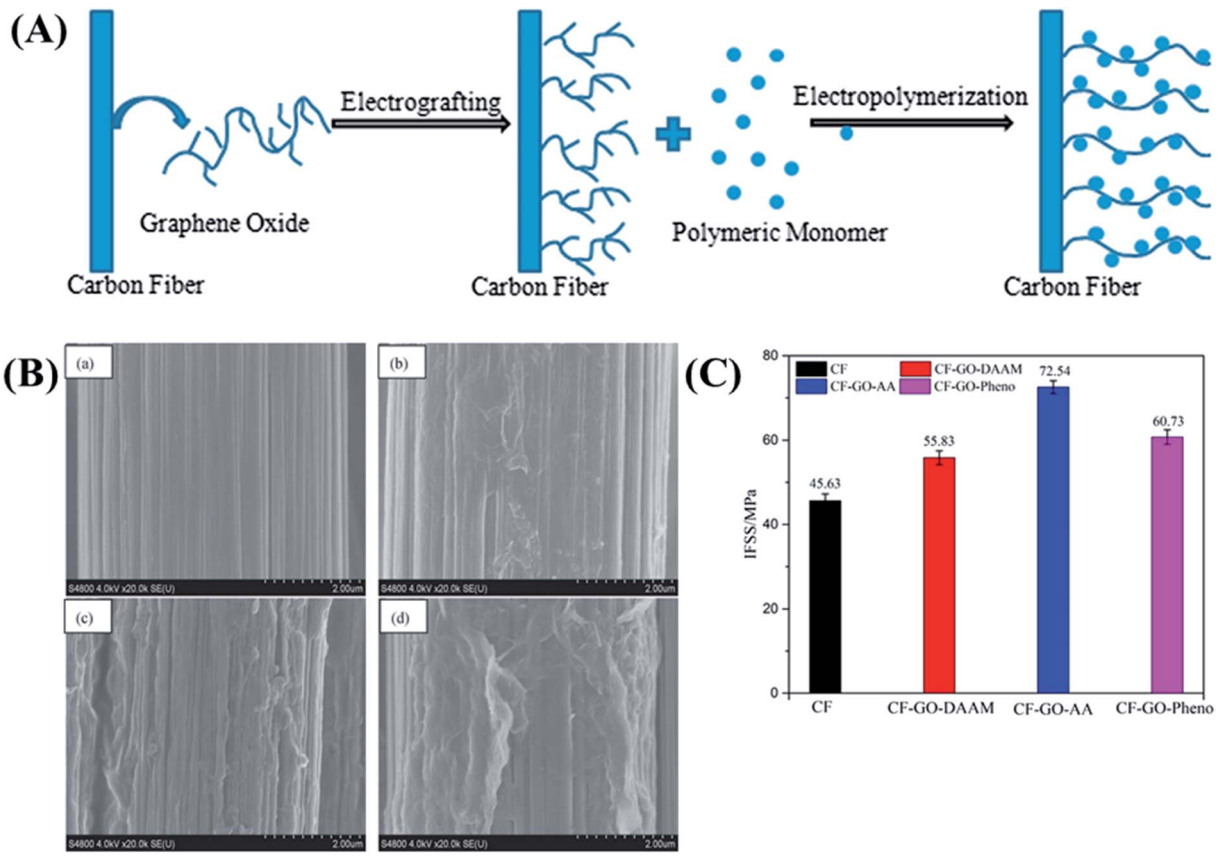

Fig. 6 (A) Schematic of electrodeposition of GO and the polymeric monomer over carbon fibers. (B) SEM images showing the surfaces of (a) untreated CFs, (b) CF–GO–DAAM, (c) CF–GO–AA, and (d) CF–GO–phenol. (C) Improvement in ILSS properties with surface modification.[79] Reproduced from ref. 79 with permission from RSC (2019).

determine the concentration of the basic functional groups on the surface.

2.3.2. Polymeric functionalization over carbon fibers. Wen *et al.*[79] worked on electrodeposition of GO and three different kinds of comonomers, including diacetone acrylamide (DAAM), acrylic acid (AA) and phenol, onto CF surfaces. The CF tows were placed as the anode in a graphene electrolytic solution with a graphite plate as the cathode followed by the monomers' electrochemical polymerization at different current densities and times. An increase in both the polar and dispersive components of the surface free energy along with a decrease in the contact angle assisted in better adhesion of the matrix over the CFs. Compared with the untreated CFs, the IFSS of CF–GO–AA reinforced composites increased from 45.6 MPa to 72.5 MPa. This remarkable increase could be attributed to the significant changes in CFs' microphysical and chemical structure after the electro-polymerization. The IFSS values of the CF–monomer (without GO) reinforced composites also were lower by 14.5%, 20.9%, and 16.8%, respectively, than that of the CF–GO–monomer reinforced composites, which indicated that the presence of GO could enhance the final interfacial properties of CFRE composites. The process of electro-functionalization of the CFs resulting in an increase in surface roughness and their corresponding improvements in interfacial properties are shown in Fig. 6.

Shi *et al.*[80] functionalized CF surfaces with a hydroxyl-terminated hyperbranched polymer (HTHBP) through a one-pot polycondensation between isophorone diisocyanate (IPDI) and tris(hydroxymethyl)aminomethane (TOAM). CFRE composites were prepared by hot compression molding. A drastic decrease in the contact angle both in polar water and in non-polar diiodomethane was observed after functionalization. Similarly, the increase in surface energy after functionalization was attributed both to the polar groups and the increase in fiber surface roughness. The IFSS value as obtained from the monofilament debonding test of sized CFRE composites was 56.8 MPa. After HTHBP treatment, compared with the untreated CFRE composites (48.8 MPa), the CF–HTHBP composites had an IFSS value of 87.8 MPa, *i.e.*, an increase of 79.9%. Furthermore, the ILSS value of the sized CFRE composites was 66.3 MPa. Compared with the untreated CF composites, the CF–HTHBP composites showed a maximum increase of 39.6% from 58.6 MPa to 81.8 MPa. At the same time, the impact strength of the CF–HTHBP composites was 76.9 kJ m^{-2}, an increase of 38.1% and 31.5% over that of the untreated CFs (55.7 kJ m^{-2}) and CF–COOH (58.5 kJ m^{-2}). The strong chemical interaction between the hyperbranched structure and the epoxy matrix assisted in proper crack energy dissipation, thereby raising the impact toughness of the system. In another paper, Andideh *et al.*[81] synthesized and grafted hyperbranched polyurethane (HBPU) over CF surfaces. Following grafting, the hydroxyl-terminated polyurethane was amine-functionalized for compatibility with the epoxy matrix. The ILSS value of CF-*g*-HBPU-OH was higher than that of CF–COOH (88.6 ± 3.9 *vs.* 72.1 ± 1.5 MPa). This is related to the diffusion and mechanical interlocking of the epoxy and HBPU chains in the interphase layer. The ILSS of CF-*g*-HBPU-NH_2 was the highest (107.2 ± 5.8 MPa), with an increase of 49% compared to that of CF–COOH. It is believed that the amine groups grafted onto the CF surface contribute to the crosslinking reaction and enhance ILSS.

Zhao *et al.*[82] grafted melamine over CFs and studied their benefits in interfacial property enhancement. The CFs were acyl chloride functionalized and placed in a stainless-steel autoclave in melamine solution (ethanol). Surface functionalization treatment was done at 553 °C for 5, 15, 25, and 35 min, respectively. IFSS was measured *via* a microdroplet debonding test. It increased by 12.1%, 28.0% and 41.3% for 5, 15 and 25 min treatment, respectively. This was attributed to the formation of considerable chemical bonding between the amine groups of melamine and the epoxy matrix. However, for 35 min treatment, the IFSS of the composite showed a decrease, which was attributed to the "over-coverage" of melamine onto CFs. The ILSS values also exhibited the same trend with a maximum of 36.4% increase for 25 min treatment. Furthermore, the composites' toughening efficiency indicated that the melamine interface could induce some smaller cracks to

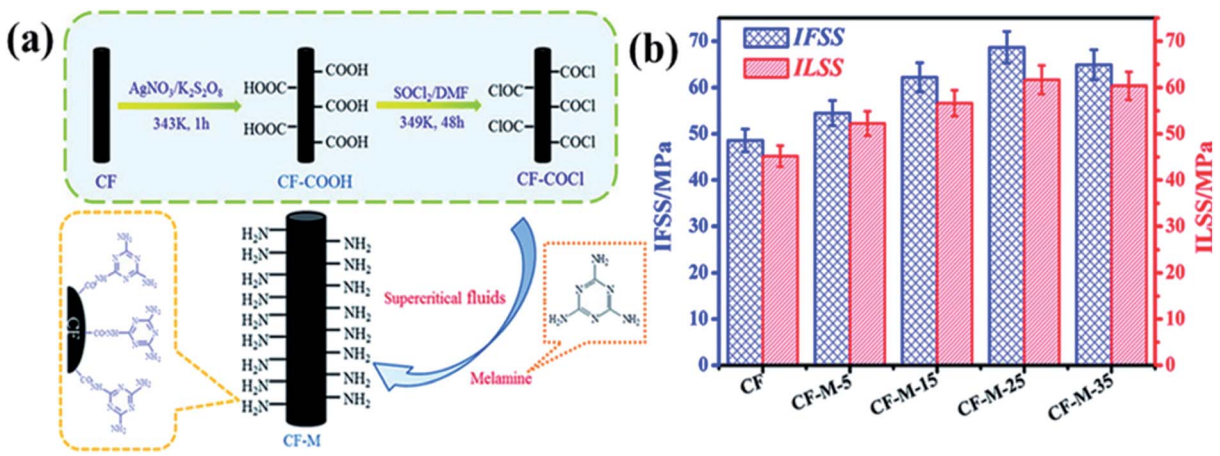

Fig. 7 (a) Schematic of the chemical functionalization of melamine over carbon fibers and (b) improvement in IFSS and ILSS properties with grafting time.[82] Reproduced from ref. 82 with permission from RSC (2016).

prevent the crack tips from contacting the fiber surface directly and make the crack path deviate away from the CF surface to the interface region. Therefore, the composite's impact strength was increased. The deposition of melamine through covalent functionalization over the CF surface and the corresponding increase in both IFSS and ILSS properties are shown in Fig. 7.

Aljarrah *et al.*[83] worked with nylon nanofibers (NF) electrospun over CFs as an interface and fabricated laminates *via* the VARTM process. It was observed that with an increase in the interfacial layer thickness, which increased with the electrospinning time, the interlaminar properties decreased. Three-layer configurations were used: nanofibers electrospun on one CF sheet and nanofibers electrospun on two opposing CF sheets with different thicknesses. The nanofiber layer was electrospun directly on the CF fabric before laminate production, which resulted in better adhesion between the NF interleaves and the CF sheets. An improvement in interlaminar fracture toughness for all three configurations was observed up to 25%. The average interlaminar fracture toughness was found to be highly dependent on the interleaved layer thickness. Maximum improvement was found when two thin opposing layers of nylon 66 NF were inserted on the delamination plane. The fractographs showed crack tip bridging and fiber interlocking at the crack surface. Further increase in the interleaved layer thickness resulted in a reduction of fracture toughness due to the formation of a new interface evident from the fractograph analysis of the crack surface.

Kim *et al.*[84] coated polydopamine (PDA) over CFs for interfacial property assessment. For this, dopamine was dissolved in a Tris–HCl buffer solution with a pH of 8.5. The buffer solution was prepared by adding 1 M HCl to a Tris solution, and the pH was monitored using a pH meter. The CFs were dipped in the PDA solution to form polymer-coated CFs. Furthermore, the coated CFs were surface treated with KH550 by dipping the grafted CFs in aqueous solutions of KH550 (2.5 wt%, pH 9–10) at 50 °C under uninterrupted stirring for 24 h. Li *et al.*[85] followed the same protocol for grafting PDA over CFs. Laminates were fabricated *via* the VARTM process. Compared with the pure epoxy (EP) resin, the flexural modulus and flexural strength of EP/CF, EP/CF–PDA, EP/CF–PDA–KH550 and EP/CF–(PDA + KH550) were observed to increase by 30.4%, 42.7%, 57.3%, 69.4%, and 10%, 15.6%, 24.9%, 34.5%, respectively. The presence of a stronger interface with better chemical compatibility with the epoxy matrix due to the presence of amine functional groups led to better interfacial properties. The process of grafting PDA over the CFs and the subsequent amine treatment are shown in Fig. 8. The corresponding improvement in both the maximum load and mechanical properties is also shown in the same figure.

Chen *et al.*[86] researched on assembling poly(-cyclotriphosphazene-*co*-4,4′-sulfonyldiphenol) nanotubes (PZSNTs) onto the CF surface as a novel multi-scale hybrid reinforcement through *in situ* template polymerization, and assessed the interfacial behavior changes of the resultant laminates. A decrease in contact angle and an increase in surface energy were obtained after the polymeric modification over the CFs. The IFSS of CF–PZSNT/EP significantly increased by 26.4%. In comparison to the as-received CFs with

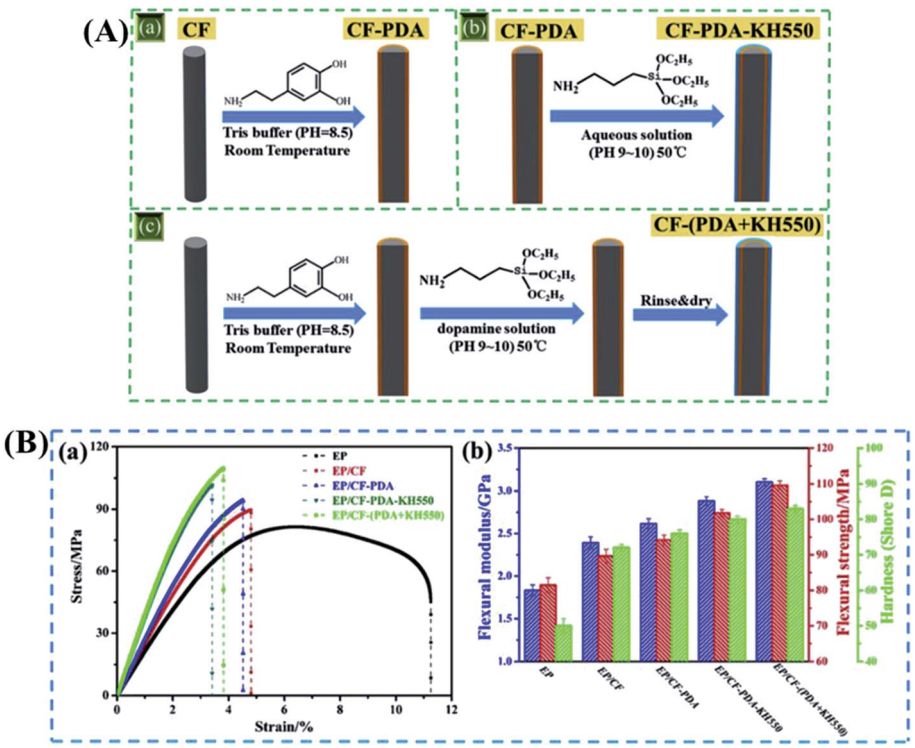

Fig. 8 (A) Schematic of step-by-step functionalization of carbon fibers with PDA and PDA–KH550 (amine). (B) The stress–strain curves (a) and flexural modulus, flexural strength and hardness (b) of pure epoxy and its composites.[84] Reproduced from ref. 84 with permission from Elsevier (2019).

Table 3 Mechanical property improvement for various polymeric modifications to the fibers in carbon fiber epoxy composites

Sl no.	Polymeric modification	Mechanical properties	Improvement over the control sample	Ref.
1	GO–diacetone acryl amide + acrylic acid + phenol	IFSS (microbond test)	58.9%	79
2	Hydroxy terminated hyperbranched polymer	IFSS (monofilament debonding test) ILSS Impact strength	79.9% 39.6% 38.1%	80
3	HBPU (1) –OH functionalized (2) $–NH_2$ functionalized	ILSS	22.8% 49%	81
4	Melamine	IFSS (microdroplet test)	41.3% (25 min treatment)	82
5	Nylon nanofibers	Interlaminar fracture toughness	25%	83
6	Polydopamine-amine functionalized	Flexural modulus Flexural strength	69.4% 34.5%	84
7	Poly(cyclotriphosphazene-*co*-4,4′-sulphonyldiphenol) nanotubes (PZSNTs)	IFSS (single fiber microbond test)	26.4%	86

commercial sizing, the IFSS of the CF–PZSNT/EP composite also increased by 18.5%. The results showed that the PZS hybrid coating was comparable to the commercial sizing on the received fibers' surfaces. The interfacial improvement might be attributed to the synergistic effect of the better wettability and compatibility, the enhanced mechanical interlocking, and the more chemical bonds between the fibers and matrix. The significantly improved surface energy could result in better wettability between the CF–PZSNT and resin, and diminish the defects at the interface of the composite. Moreover, the PZSNTs can stick to the epoxy matrix and work as an anchor to improve the mechanical interlocking effect. Plenty of phenolic hydroxyl groups (Ph-OH) on CF–PZSNT surfaces also reacted with epoxy and resulted in an increased cross-linking density in the interphase region, and hence, the interfacial adhesion strength was greater than the cohesive strength of the resin. It should be noted that the mechanical interlocking may play a key role in improving the interfacial properties. A summary of the above results is presented in Table 3.

2.3.3. Carbonaceous particle modification of carbon fibers. In the work done by Dong *et al.*[87] carbon black nanoparticles were grown over CFs through chemical vapor deposition. The process involved fixing the CFs over a graphitic flame with tension at both the ends. Next, the entire set-up was placed inside a quartz tube furnace under a constant flow of N_2 gas. The temperature was subsequently increased at a constant rate and ethanol was passed through the furnace to grow the carbon black (CB) over the CFs. After the growth of CB, the reactor was allowed to cool down and the samples were coded as untreated CF and CF-*X* min (where *X* corresponds to the growth time of the CB). The IFSS of CF-5 min considerably rose from 49.45 MPa to 71.91 MPa by 44.4% in comparison to that of the untreated CFs. With further increase of CB growth time, the IFSS of CF-10 min decreased to 54.1 MPa. Although the fibers' roughness and wettability were improved, the instability of the secondary structure of CB made the microdroplet composites slide easily from the fiber surface for the CF-10 min sample.

Batista *et al.*[88] formed a carbon-nanocrystal (CNC) slurry with 12.2 wt% amine-functionalized CNC in water. The sizing agent was prepared by adding the CNC suspension to epoxy and the curing agent with continuous stirring and suspension. CNCs were set at concentrations of 0.6 wt%, 1.0 wt%, and 2.0 wt% to the total-sizing solution. CFs were sized by two different techniques for comparison purposes. The first technique consisted of dipping a 12k filament tow into the sizing solution for 20 s and slowly pulling the tow out. The second technique consisted of aligning and mounting individual CFs onto a square-shaped metal frame and immersing them into the sizing solution for approximately 32 min (sequence of 5 min without stirring followed by 3 min with stirring) and in the last minute slowly pulling the metal frame out. The single fiber fragmentation test (SFFT) showed the optimal sizing concentration as 1.0 wt% APTES-CNCs in the sizing which led to an IFSS increase of 77% and 81% for the 12k tow sized CFs and individually sized CFs, respectively, as well as an improvement in the failure mode. The CFs sized at 2.0 wt% APTES-CNCs exhibited an increase of 54% for the 12k tow sized CFs and a reduction of 8% for the individually sized CFs. This indicated that the excessive sizing generated multilayers of CNCs that could cause slippage of the nanoparticles with respect to each other and decreased the efficiency of stress transfer at the interphase. Micrographs of the birefringence stress patterns indicated that the fracture of unsized CFs occurred mostly by frictional de-bonding. It is the characteristic of weak interfaces and results in low IFSS. In contrast, for the APTES-CNC sized CFs there was no obvious debonding. Instead, the birefringence patterns for CFs sized with nanoparticles were characteristic of very strong adhesion and a well-bonded interphase, evidenced by the extensive crack propagation into the matrix, which correlated with the highest level of adhesion at the interphase. The scheme of fibers modified through sizing and its effect on the resulting composites are shown in Fig. 9.

Zhang *et al.*[89] studied the interfacial effects of CNT-sized CFRE composites. CNTs were both acid and amine-functionalized in separate batches. The CNT–COOH sized CFRE composites exhibited improvements of 10%, 27%, and 59% in IFSS, ILSS, and flexural strength, respectively, compared with the commercial CFRE composites. The CNT-NH_2 sized CFs

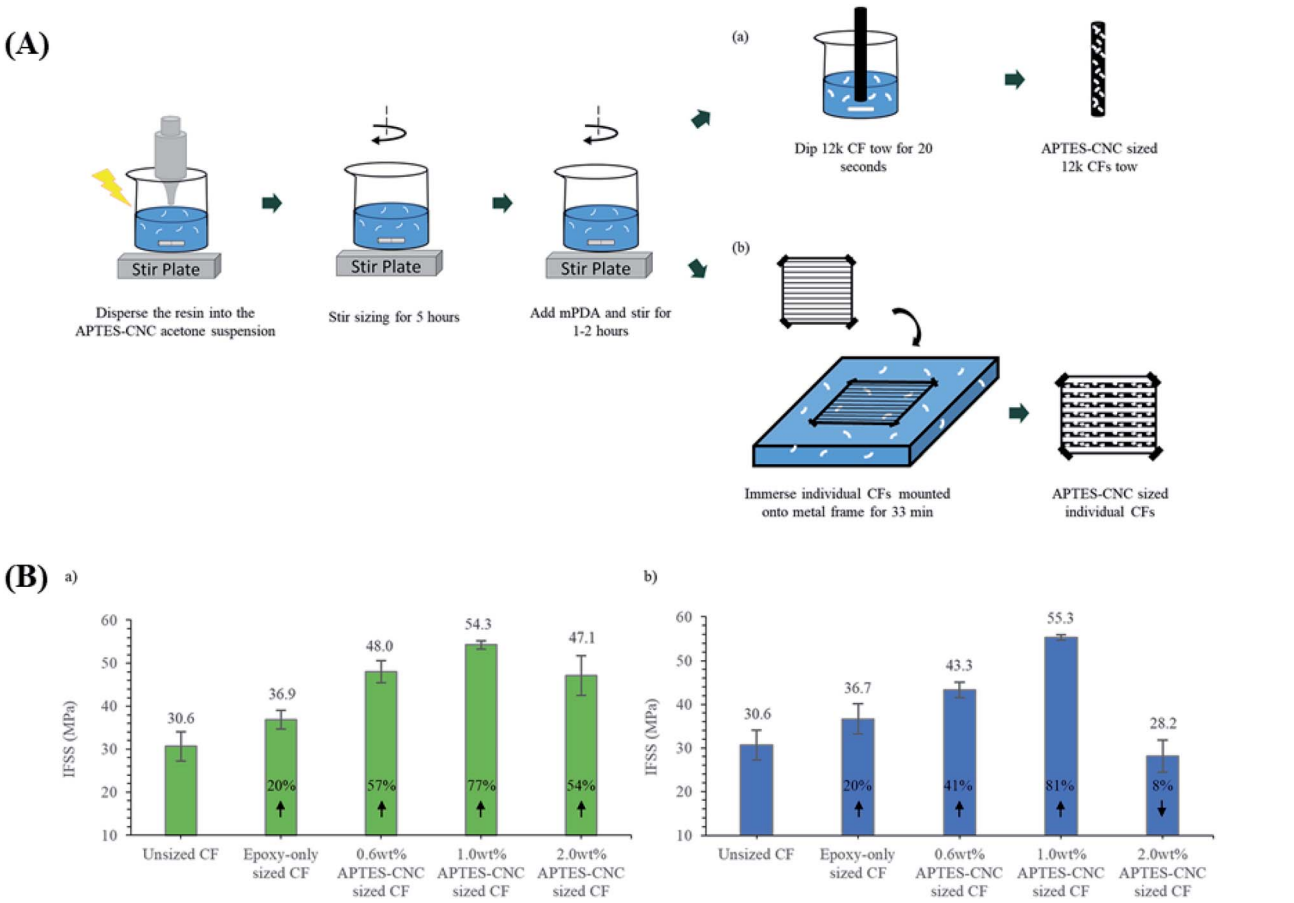

Fig. 9 (A) Fabrication of the hybrid laminate CNC-sized carbon fibers and (B) improvement in the ILSS and IFSS properties of the resulting composites.[88] Reproduced with permission from Elsevier (2018).

had adverse effects on IFSS and ILSS, and the improvement of the flexural properties was smaller than that for CNT–COOH.

Yao *et al.*[90] presented work on growing CNTs over CF surfaces using chemical vapor deposition. CFs were first de-sized and then oxidized with hydrogen peroxide. The oxidized CFs were immersed in a catalyst solution containing ferric nitrate ($Fe(NO_3)_3 \cdot 9H_2O$) and cobalt nitrate ($Co(NO_3)_2 \cdot 6H_2O$) in ethanol with a molar ratio of 1 : 1 for 10 min. Catalyst coated CFs were placed in a CVD furnace under a N_2 atmosphere. The temperature was increased in steps and C_2H_2 and H_2 gas were purged inside the chamber at a constant ratio. Following the reaction, the chamber was degassed to vacuum. The laminates for ILSS measurements were prepared *via* the prepreg technique and the samples for IFSS measurement were prepared *via* a single-filament pull out test. The coating of CNTs visibly increased the roughness and subsequently improved the wettability of the fabrics. It was observed that the ILSS and IFSS of the CNT-coated CFRE composites increased by 32.3% and 30.7%. At the same time, significant improvement in dielectric permittivity and conductivity by the addition of CNTs was also reported.

Li *et al.*[91] followed a similar protocol to grow CNT aerogels over CFs. An Ar–H_2 mixture (volume ratio of 1 : 1) was also injected as a carrier gas at a rate of 4000 sccm. The nanotubes spontaneously formed continuous sock-like aerogels in the gas flow under these synthesis conditions, which can be blown out with the carrier gas. A rotating mandrel continuously winded the CNT aerogels and they were densified by *in situ* liquid-spraying of ethanol–water solution. The pristine CNTs had 3–7 walls with an average diameter of 6–10 nm. In this study, the CNT films were treated using *m*-chloroperoxybenzoic acid (*m*-CPBA) before their hybridization with CFRE laminates. The ultrathin CNT films increased the ILSS of the composites by 5%, but the thicker CNT films reduced the ILSS slightly. Moreover, the interlayer ultrathin CNT films dramatically improved the compression strength of the hybrid composite by 34% compared to that of CFRE laminates, while the thick CNT films led to an improvement of 19%. The SEM morphologies indicated a high compression load-bearing capacity of the CNT modified CFs, thereby changing their failure mode.

Chen *et al.*[92] modified CFs with a liquid phase deposition strategy. Here, expanded graphite (EG) was formed at a high temperature by inserting graphite into a pre-heated furnace to 1000 °C for 1 min. The EG was dissolved in an acetone solution and CFs were dipped in the solution to deposit the EG over the CF surface. The EG bath was prepared at different concentrations of the nanoparticles (0.1, 0.3, 0.5, 1.0, 1.5, and 2.0 wt% relative to that of composites). The laminates were prepared *via*

the VARTM technique. The carbon element showed a graded dispersion in the interface region, and a gradient interface layer with the modulus decreasing from the fibers and matrix was found to be built. An increase in the ILSS of 28.3% for unidirectional CFRE composites was observed with an EG loading of 1 wt%. The flexural properties of the composites were also enhanced owing to the improved interfacial performance. When the EG loading exceeded 1.5 wt%, both ILSS and flexural strength decreased, which may be attributed to the reappearance of stress concentration induced by the agglomeration of excess EG.

In a similar method, Zhang *et al.*[93] prepared a GO sizing over CFs in a sizing solution. The aqueous dispersion of GO (5 mg ml^{-1}) was added to epoxy emulsions with GO contents of 0, 1, 2.5, 5, 7.5 and 10 wt%, which were represented as GO0, GO1, GO2.5, GO5, GO7.5, and GO10, respectively. The virgin CFs were pulled through the GO-modified sizing and subsequently dried at 100 °C. It was found that the IFSS of GO modified CFs was much higher than that of commercial-SCF, particularly SCF–GO7.5 fibers exhibiting an increase of 70.9% in comparison to CF fibers and about 36.3% in comparison to SCF–GO0 fibers. The SCF–GO5–EP composite was found to have the highest ILSS of 51.3 MPa, an increase of 12.7% compared to that of the SCF–GO0–EP composite (control composite). However, a further increase in GO loading from 5 to 10 wt% led to only slight changes in ILSS. It was observed that the GO-modified composites showed crack propagation through both the fibers and matrix, while the interface was intact, indicating an improved interfacial bonding. Fig. 10 indicates how the GO-sizing modification enhanced the fiber's surface compatibility with the matrix, in turn, improving the interfacial behavior.

Jiang *et al.*[94] deposited GO over CFs *via* electrochemical and electrophoretic deposition. The ILSS and compressive strength of the composites increased by 59.4% and 12.8%, respectively. Ma *et al.*[95] worked on modifying GO nanosheets chemically with cyanuric chloride (TCT) and diethylenetriamine (DETA). Then, quantitative GO–TCT–DETA was added to epoxy/toluene solution with GO–TCT–DETA contents of 0.1, 0.5, 1.0, and 1.5 wt%.

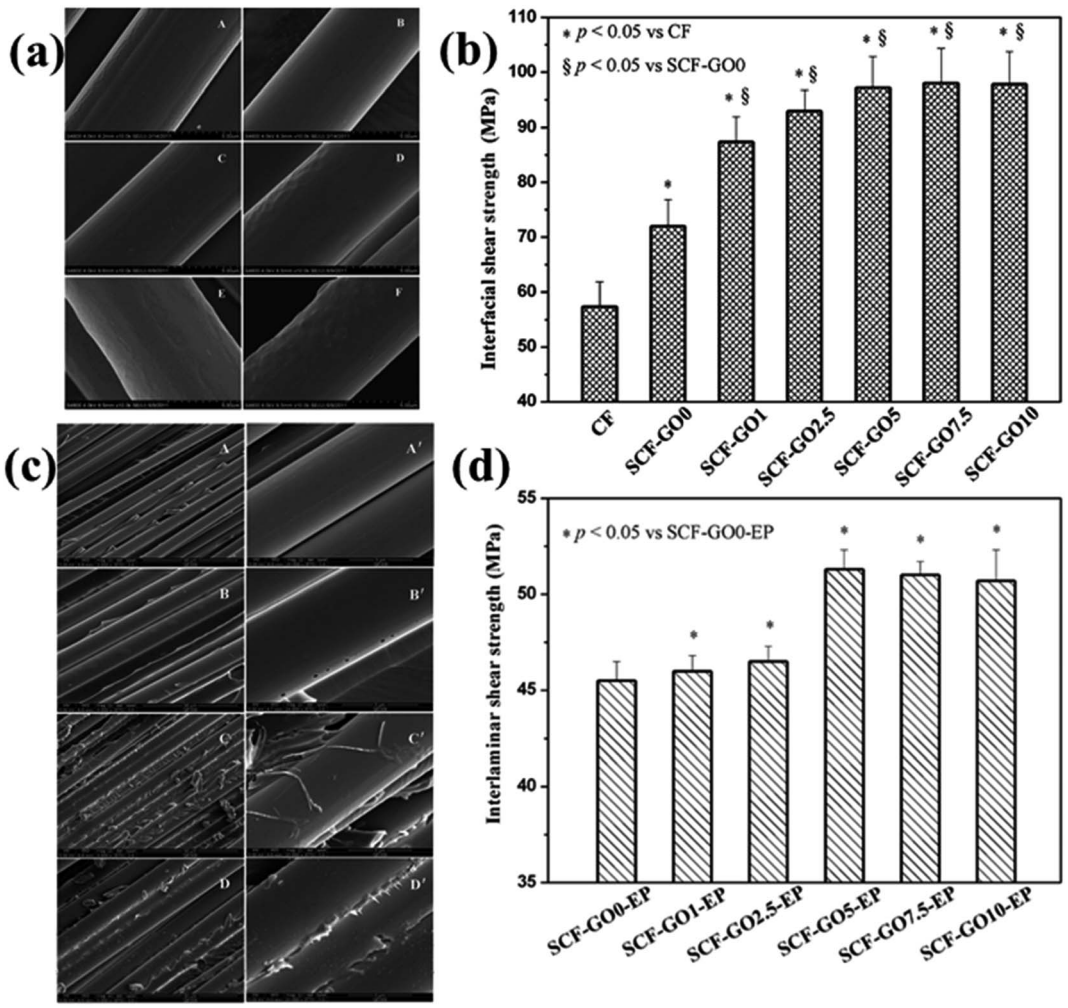

Fig. 10 (a) SEM images of carbon fibers after GO modified sizing treatment: (A) T700S; (B) virgin carbon fibers (CFs); (C) SCF–GO0; (D) SCF–GO1; (E) SCF–GO5; and (F) SCF–GO10. (b) IFSS of the resulting composites; (c) fracture surface micrographs of carbon fiber/epoxy composites: (A and A′) SCF–GO0–EP; (B and B′) SCF–GO1–EP; (C and C′) SCF–GO5–EP; (D and D′) SCF–GO10–EP; (d) ILSS of the resulting composites.[93] Reproduced from ref. 93 with permission from ACS (2012).

Table 4 Mechanical property improvement for fiber modifications with carbonaceous nanoparticles in carbon fiber–epoxy composites

Sl no.	Fiber modification agent		Mechanical properties	Improvement over the control sample	Ref.
1	Carbon black		IFSS (micro-composite test)	44.4%	87
			ILSS	22%	
2	Carbon nanocrystals	(1) 12k tow sized	IFSS (SFFT)	77%	88
		(2) Individually sized		81%	
3	CNT–COOH		IFSS (SFFT)	10%	89
			ILSS	27%	
			Flexural strength	59%	
4	CNTs		IFSS (SFFT)	32.29%	90
			ILSS	30.73%	
5	CNT-aerogels	(1) Ultra-thin	ILSS	5%	91
			Compressive strength	34%	
		(2) Thicker	ILSS	Reduction	
			Compressive strength	19%	
6	Exfoliated graphite		ILSS	28.3%	92
7	GO-epoxy sizing		IFSS (microbond test)	70.9%	93
			ILSS	12.7%	
8	Electrodeposited GO		ILSS	59.4%	94
			Compressive strength	12.8%	
9	Triazine derivative functionalized GO sizing agent		IFSS (monofilament debonding test)	104.2%	95
			ILSS	100.2%	
			Flexural strength	78.3%	

CFs were impregnated with the modified sizing agent. A uniform distribution of GO sheets on the CF surface and the enhancement of surface roughness were obtained. Moreover, significant enhancements, *i.e.*, 104.2%, 100.2%, and 78.3%, in IFSS, ILSS, and flexural strength were achieved in the composites with only 1.0 wt% GO–TCT–DETA sheets introduced in the fiber sizing. The GO–TCT–DETA in the interface region effectively enhanced the stress transfer and relieved the local stress concentrations. A summary of the above results is presented in Table 4.

2.3.4. Metals and metal oxides. Metal oxides/nitrides are used with several other reinforcements to form hybridized composites. Yan *et al.*[96] worked on the deposition of metallic copper and MWCNTs over CFs through subsequent

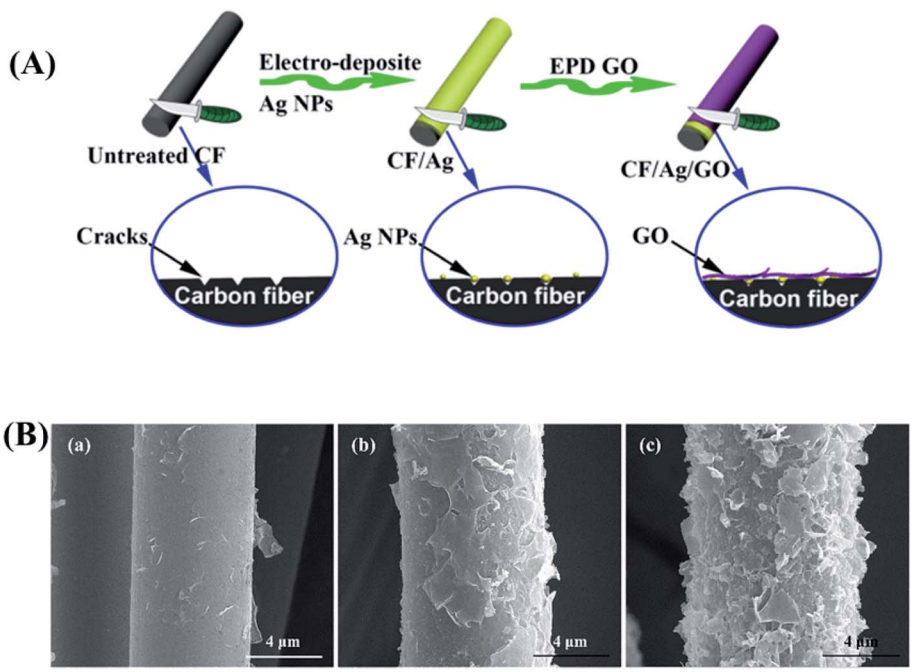

Fig. 11 (A) Schematic of surface modification of carbon fibers with Ag/GO and (B) SEM micrographs showing the increase in surface roughness with subsequent modifications.[97] Reproduced from ref. 97 with permission from Elsevier (2017).

electrophoretic deposition (EPD) processes. It was observed that the Cu and CNTs formed conduction pathways as well as increased surface area and roughness. The thermal conductivity and ILSS of the CNTs–Cu–CF/epoxy composites increased by 292% and 39.5%, respectively, compared with those of the CF/epoxy composites.

Wang *et al.*[97] developed two-layered hybrid CFs with Ag nanoparticles/GO CFs by an electrochemical deposition followed by electrophoretic deposition. The resulting modified CFs were marked as CF/Ag/GO-30, CF/Ag/GO-60, and CF/Ag/GO-90, respectively, according to their electro-deposition time in seconds. It was observed that the IFSS and tensile strength increased by a maximum of 86.1% and 36.8%, respectively for CF/Ag/GO-60 laminates. The presence of GO increased the surface roughness and the number of active functional groups. GO could enhance wettability and then enhance the interfacial interaction of CFs and epoxy. However, when the deposition time was over 60 s, the IFSS value started to decrease because of the weak van der Waals interaction among GO sheets leading to interface failure in the heavy layer of the GO sheets. The scheme for the CF surface modification and the corresponding micrographs are shown in Fig. 11.

TiO_2 has been grafted over CFs by various methodologies, and several researchers have analysed their effect on the interfacial properties. Ma *et al.*[98] grew TiO_2 nanorods (NRs) over CFs by hydrothermal and supercritical methods. A TiO_2 sol was formed in ethanol solvent and the acid-functionalized CFs were pulled through the sol and kept in an oven at 373 K for half an hour. The cycle was repeated four times. Next, TiO_2 nanowires (NWs) were grown onto CFs by a hydrothermal method, and TiO_2 NRs were grown onto CFs in supercritical water. After growing TiO_2 NRs by the hydrothermal and supercritical methods, CF composites' interfacial strength increased significantly. The IFSS of CF–COOH–TiO_2 NRs exhibited an increase of 38.0% and 17.0% over the untreated CFs and CF–COOH, respectively. The IFSS of the CF–COOH–s-TiO_2 NRs exhibited an increase of 52.4% over the untreated CFs. The improvement can be ascribed to two aspects, the enhancement of the mechanical interlocking effect caused by the permeation of needle-like TiO_2 NRs with high specific surface area into the resin matrix, and the good wettability with the resin matrix resulting from TiO_2 NRs with abundant hydroxyl groups. This is consistent with other nanoparticle enhancements, such as GNPs, CNTs, and silica particles. It was observed that supercritical water accelerated the growth efficiency of TiO_2 NRs.

In another study of Ma *et al.*,[99] TiO_2 NWs were grown onto amine-functionalized CFs in supercritical water. A TiO_2 seed layer was grown over the CFs through a sol–gel technique. After the successful deposition of the seed layer, the resulting CFs were placed in an autoclave heated to 375 °C at a pressure of 22.5 MPa for 15 min. Subsequently, the hybrid CFs were washed with water and ethanol, and then sonicated. The surface energy of the untreated fibers was 30.13 mN m^{-1}. After TiO_2 NW growth, the surface energy and the components of CF–TiO_2 NWs increased. The contact angles also decreased from 87.67° to 67.66° for water and from 63.90° to 53.90° for diiodomethane. The increased polar component of surface energy could be interpreted from the increase in hydroxyl groups of TiO_2 NWs on the fiber surface. The increased dispersion component could be attributed to the fiber surface's different chemical compositions and the increased fiber surface roughness caused by TiO_2 NWs. The contact angles of CF–HMTA–TiO_2 NWs and CF–PEI–TiO_2 NWs further decreased in the test liquids, and the surface energy increased to 68.05 mN m^{-1} and 71.36 mN m^{-1}, respectively. The IFSS of CF–s-TiO_2 NWs exhibited an increase of 15.3% compared to that of the untreated CFs. The IFSS values of CF–COOH–TiO_2 NWs, CF–HMTA–TiO_2 NWs and CF–PEI–TiO_2 NWs were 93.3, 112.1 and 122.4 MPa, respectively, which were higher than those of CF–COOH (76.6 MPa), CF–HMTA (98.5 MPa) and CF–PEI (100.3 MPa), respectively. The improvement can be attributed to four aspects: (i) the polarity of TiO_2 NWs is similar to that of the carboxyl and amino on the CF surface, which could enhance the affinity between CFs and TiO_2 NWs; (ii) the enhancement of mechanical interlocking caused by the permeation of high surface area and needle-like TiO_2 NWs into the resin matrix; (iii) the good wettability with the resin matrix resulting from TiO_2 NWs with abundant hydroxyl groups; and (iv) a more distinguished gradient between the fiber and matrix, thus reducing stress concentration at the interface and absorbing more failure energy.

Xiong *et al.*[100] came up with thiol–ene click chemistry to graft nano-sized TiO_2 over CFs. TiO_2 was amine-functionalized followed by vinyl functionalization. CFs were acid-functionalized followed by amine functionalization. The click reaction between CF–KH590 and vinyl TiO_2 was performed at room temperature for 30 min by irradiation with 365 nm UV light. Compared to the raw CF/epoxy composites, the composites reinforced by the CFs grafted with nano-TiO_2 showed an improvement of 78% in IFSS. The introduction of nano-TiO_2 significantly enhanced the surface energy of fibers and increased the wettability and mechanical interlocking between the fibers and resin, resulting in a significant increase in the interfacial properties of composites. However, the tensile strength and flexural strength slightly decreased, which was attributed to the surface damage of CFs caused by nitric acid treatment. Compared to the oxidized CF/EP composites, the CF–KH590/EP (amine treated CF) composites exhibited an increase in mechanical properties due to the introduction of a silane coupling agent. After grafting nano-TiO_2 onto the surface of CFs, the tensile strength and flexural strength of CF–TiO_2/EP composites increased by 39.6% and 32.3%, respectively. The improvement in properties upon the addition of TiO_2 was attributed to the increase in surface asperity of the CFs, leading to an increase in the frictional forces between the fibers and the matrix. The unique method of grafting functionalized particles onto CFs *via* thiol–ene click chemistry is simple and rapid, and hence quite efficient.

Fakhrhoseini *et al.*[101] proposed growing magnetite (Fe_3O_4) nanoparticles on the surface of CF tows by dipping them in an ammonium iron sulfate solution and subjecting them to subsequent heat treatment in a tube furnace under a N_2 atmosphere. The ILSS increased by 31.1% due to the mechanical interlocking at the fiber–resin interface as a result of magnetic nanoparticles' presence, which was verified by contact

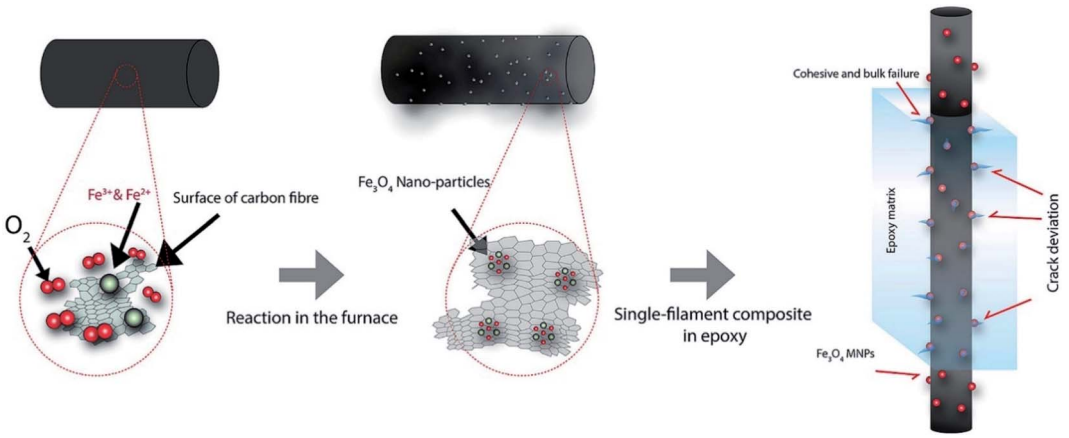

Fig. 12 Schematic of Fe_3O_4 nanoparticle growth over carbon fibres and their subsequent effect of better mechanical interlocking with epoxy.[101] Reproduced from ref. 101 with permission from Elsevier (2019).

angle and surface energy analysis. The dispersive component of the surface energy was increased for magnetite deposited CFs indicating a higher affinity for epoxy adherence and a stronger interface. The scheme for Fe_3O_4 growth over carbon fibres and the mechanism for mechanical interlocking with the matrix are illustrated in Fig. 12.

Jin *et al.*[16] grew $Ni(OH)_2$ nanosheets over CFs by submerging unsized CFs in a beaker containing 0.1 M $Ni(NO_3)_2 \cdot 6H_2O$, 500 mg of urea, and 200 ml of deionized water. Depending on the time of reaction (1 h, 2 h, 3 h, and 4 h), the modified CFs were named NCF1, NCF2, NCF3, and NCF4, respectively. The VARTM process was used to fabricate the laminates. For NCF0, the IFSS value was 45.8 MPa, while the IFSS values of NCF1 and NCF2 increased by 26.2% and 52.6%, respectively. After deposition of the $Ni(OH)_2$ nanosheets, the ILSS curves showed a zig-zag pattern over a larger range of strain, indicating that the crack propagation was disturbed by the presence of the nanosheets. On the one hand, $Ni(OH)_2$ nanosheets played a role in improving the CF surface's roughness. On the other hand, the nanosheets can penetrate the resin, which makes the cracks change the propagation direction, leading to the improvement of interfacial bonding.

A summary of the above results is presented in Table 5.

The carbon fiber modifications started from the application of electrochemistry and materials science, *e.g.*, carbon fiber electrodes. Certain treatments on the inert surfaces of carbon fibers introduced several defects over the fibers, in turn deteriorating the mechanical properties of the composite. Compatible polymeric modifications increased interfacial interactions strongly but raised new issues of intrinsic porosity, stability, and strength of additional interfaces in the case of thicker coatings. To limit the complicated chemistry involving polymerization over carbon fibers, direct deposition of nanoparticles came into the picture. Dip-coating, chemical vapor deposition, physical vapor deposition, electrochemical and electrodeposition are to name a few. Direct particle deposition not only improved the surface roughness but also developed a mechanical interlocking with the matrix. However, the exact estimation of the concentration of particles being deposited on that fiber is uncertain leading to wastage of nanoparticles present in the suspension. Furthermore, since structural integrity of the fibers determines several mechanical properties such as tensile strength and modulus, there continues to exist the need to perform surface treatments without hampering the original strength of the CFs. More recently, development of new architectures of nanoparticles over CFs in the shape of nanorods or -wires has significantly improved the interfacial

Table 5 Mechanical property improvement for fiber modifications with metal/metal oxide fillers in carbon fiber–epoxy composites

Sl no.	Fillers	Mechanical properties	Improvement over control samples	Ref.
1	Metallic Cu + MWCNTs	ILSS	39.5%	96
2	Ag + GO	IFSS (microbond test)	86.1%	97
		Tensile strength	36.8%	
3	TiO_2 NRs	IFSS (microbond test)	38%	98
4	TiO_2 NWs	IFSS (microbond test)	15.3%	99
5	TiO_2 grafted *via* thiol–ene click	IFSS (microbond)	78%	100
		Tensile strength	39.6%	
		Flexural strength	32.3%	
6	Fe_3O_4	ILSS	31.1%	101
7	$Ni(OH)_2$	IFSS (microbond test)	52.6%	16

interactions through directly impinging into the epoxy and strengthening the mechanical bonding with the matrix. Such directional nano-growths generate better surface area for adhesion with the matrix and substantially reduce the issue of particle agglomeration. Therefore, research into fiber-based modifications for improved interfacial interactions is gradually gaining momentum.

3. Self-healing abilities of fiber reinforced polymers (FRPs)

Fiber reinforced polymers (FRPs) undergo several modes of failure resulting in high maintenance cost, replacement after damage, and the risk of catastrophic failure during service. The approach of self-healing in such structures has recently attracted some attention. Self-healing in a polymeric material refers to the onset of cross-linking or chain entanglements by chemical or physical means triggered by an external agent (mechanical, thermal, chemical, *etc.*).[23,102–106] In the case of FRPs, external stress is predominantly mechanical and thermal. This section will be limited to the discussion of self-healing after the application of mechanical stress to the composites. The most common problem in FRPs is the damage of the polymer matrix/fiber interface and the phenomenon of microcracking in the matrix. The broad approach to achieve self-healing ability in FRP systems is introducing micro or nano-sized polymeric containers filled with healing agents.[107] The aim is to arrest the propagation of cracks in the composites. The crack during propagation causes rupture of the containers and the release of healing agents from them. The healing agents fill the crack by capillary action and react to polymerize or cross-link, thereby healing the crack. This approach of self-healing is extrinsic in nature because external healing agents are added to the material for the healing process. There is another approach for intrinsic self-healing where the material uses its inherent ability to heal after being activated by an external stimulus (*e.g.* heat).[102] The method is mainly targeted to heal the de-bonded interface between the fibers and matrix. The fibers and matrix are chemically modified to form a thermo-reversible covalent bond. The covalent bond breaks into reactant species during mechanical interfacial failures, and on heating, the reactant species again react to form covalent bonds thereby healing the interface of the fibers and matrix. Therefore, the major approaches for inducing self-healing ability are to either (a) add a catalytically active reaction system or (b) introduce thermo-reversible chemical bonds at the matrix/fiber interface. The self-healing efficiency (η) is measured by quantifying the recovery of mechanical properties (fracture toughness, ILSS, fatigue, compression after impact (CAI), *etc.*) on healing after the damage,[24,108–111]

$$\eta = \left(\frac{P_f}{P_i}\right) \times 100\% \quad (2)$$

where P_i and P_f represent the corresponding mechanical properties measured before damage and after the healing cycle, respectively.

The earliest pioneering work in self-healing was conducted by White *et al.*[24] They developed microcapsules with an outer skin of a urea-formaldehyde (UF) thermoset filled with the dicyclopentadiene (DCPD) monomer dispersed in the epoxy matrix, as schematically presented in Fig. 13. The other reactant species, *i.e.*, Grubb's catalyst was mixed with the epoxy matrix prior to the addition of microcapsules in it. The authors proposed that during the crack propagation, microcapsules in the path of cracks get ruptured and the DCPD is released into the microcracks undergoing ring-opening metathesis polymerization (ROMP) in the presence of Grubb's catalyst to heal the microcracks. The crack growth was controlled during the tests, and its propagation was allowed up to the end of the specimen without rupturing it in two pieces. After the failure of the specimen, the crack was allowed to heal for 48 h at RT. The epoxy matrix's healing efficiency was quantified in terms of fracture toughness using a tapered double cantilever beam (TDCB) specimen and it was found to be 75%. This signifies that 75% of fracture toughness was recovered after the healing process. SEM images showed evidence of ruptured microcapsules having an average diameter of 220 μm.

Brown *et al.*[108] followed the same process to study the fracture toughness of a microcapsule-loaded epoxy matrix and its self-healing efficiency as a function of microcapsule size and vol%. The authors synthesized various sizes of microcapsules having average diameters of 50 μm, 180 μm and 460 μm

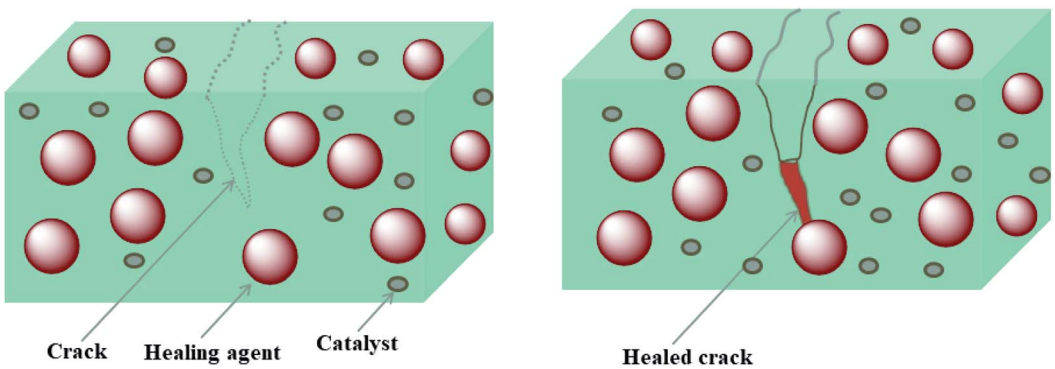

Fig. 13 Schematic depicting the concept of microcapsules and their self-healing action.

and they performed the fracture toughness tests using the TDCB specimen. They observed an increase of 127% in fracture toughness with the introduction of microcapsules. This increase was observed up to a critical vol% of microcapsule loading and then it decreased. It was also observed that the smaller size microcapsules (50 μm) required lower vol% to reach the same magnitude of fracture toughness compared to larger microcapsules. On the other hand, to achieve the same magnitude of healing efficiency exhibited by a larger microcapsule (180 μm, 5 vol%), a higher amount of smaller size microcapsules (50 μm, 20 vol%) was needed. This was due to the requirement of larger volume of DCPD for the same amount of healing. The average healing efficiency by the incorporation of both the above sizes of microcapsules (50 μm and 180 μm) was 70% after 24 h of undisturbed healing.

Rule *et al.*[109] studied the effect of the size of microcapsules and wt% loading on the self-healing properties of the epoxy matrix. The need for smaller size microcapsules was highlighted for materials having one of the dimensions much smaller (<100 μm) than other dimensions, *e.g.*, thin polymeric coatings or lamina. The average diameter of the synthesized microcapsules varied from 14 μm to 386 μm. It was observed that the recovery of fracture toughness of larger microcapsules (386 μm) was higher than that of the smaller microcapsules (63 μm) for any fixed weight fraction. SEM micrographs also showed that even at higher loading (20.5 wt%), the smaller microcapsules incompletely filled the cracks due to the shortage of the healing agent, whereas at a lower loading (10 wt%) the larger microcapsules completely filled the cracks.

In another study, Li *et al.*[110] used a dual component system of epoxy and an amine hardener as a healing agent in microcapsules. The healing agent's choice was based on the high affinity of the healing agent towards the epoxy matrix system, since both have the same chemical structure. Moreover, the epoxy resin used as the healing agent was chosen with lower molecular weight with respect to the epoxy matrix to have better processability during microcapsule formation and facilitate easy flow through the cracks. The microcapsules with a diameter of 50–62 μm have an outer skin of poly-methyl-methacrylate (PMMA). The reason for the choice of PMMA as the outer shell of microcapsules was that it does not need to be polymerized and has higher compatibility with the epoxy matrix than the UF thermoset. The fracture toughness test was conducted on the TDCB specimen and the cracked specimen was allowed to heal for 24 h at RT. The intrinsic fracture toughness of the specimen was found to increase up to 5 wt% loading and then it decreased with further loading. The maximum healing efficiency reported was 84.5% at 15 wt% loading. The reason for the high efficiency was high molecular miscibility, high flowability, and fast consolidation of the epoxy healing agent into the matrix. The above discussion leads to a conclusion that there is a need for an optimized microcapsule size and its loading in the matrix so as to get a trade-off between the increase in the intrinsic strength of the matrix by reducing the size of the microcapsule and managing strength recovery (healing efficiency) by increasing the size of the microcapsule.

3.1. Induction of self-healing abilities in CFRE laminates using microcapsules

A few years after the introduction of microcapsules in the epoxy matrix, Kessler *et al.*[111] introduced microcapsules into CFRE laminates. UF microcapsules were filled with DCPD having an average diameter of 166 μm and dispersed in epoxy resin at 20 wt%, and 5 wt% Grubb's catalyst was mixed with the epoxy resin. The CFRE laminates were manufactured with the hand lay-up compression molding technique having 16 layers of CFs. Width tapered cantilever beam (WTCB) specimens were prepared for the interlaminar fracture test. After the crack reached the tapered region, the specimen was unclamped and allowed to heal for 48 h at RT. The results showed that the average healing efficiency was 38%. The healing at 80 °C for 48 h exhibited a healing efficiency of 66%. The increase in healing efficiency at 80 °C was due to the increase in the degree of curing of DCPD at the elevated temperature.

Sanada *et al.*[112] used bigger size microcapsules (40 wt%) with the healing system of DCPD/Grubb's catalyst in the CFRE composite. DCPD was filled in microcapsules made of a UF skin with an average diameter of 211 μm. The alignment of the CFs was kept unidirectional in the composites. The specimens were tested in the transverse direction. After the specimen broke into two pieces, they were clamped shut and allowed to heal for 24 h at RT followed by 24 h at 80 °C. The healing efficiency was found to be 19%. The scattering in the mechanical test data in both the above-mentioned reports was significantly high due to microcapsules' non-uniform dispersion. The increase in viscosity due to microcapsules' addition also contributes to the non-uniform dispersion in the epoxy matrix. The loss in composites' properties may arise due to the presence of large size microcapsules and their agglomerated distribution. They can act as micro-defects and sites for stress concentration for early failure. The other reason for the low healing efficiency can be the insufficient distribution and availability of microcapsules at interfaces and near microcracks. Since there was no control of microcapsule placement in the composite, the required amount of healing agent may not be present near the damaged sites to heal the failed interfaces. One of the other disadvantages of using microcapsules was that they showed only one-time healing action at a particular place. If the healed place cracks again, there are very less chances for the presence of healing agents to heal that crack again. Therefore, different approaches were adopted to achieve healing abilities in composites for multiple cycles of damage.

3.2. Induction of self-healing abilities using micro-/nanovascular networks in the epoxy matrix and CFRE laminates

A few years after the introduction of the concept of microcapsules for self-healing, another approach for self-healing was introduced by Toohey *et al.*[113] They proposed to use a microvascular network inspired by veins and arteries in biological systems that supply the necessary biochemicals for different functions. The microvascular network was introduced as a 3D network of microtubes of diameter 220 μm for healing agents inside the composite. After the specimen fails and heals, the

healing agents can be supplied again from an external source (using a micro-syringe) to the hollow microvascular network for recharging the healing system for the next healing cycle. This approach has an advantage of multiple healing cycles, which was one of the limitations of microcapsules having one-time healing action. This healing method was primarily aimed to heal the microcracks at the interfaces. The fabrication of the 3D microvascular network was performed using the direct-write assembly method. A computer-controlled 3D printing technique used an organic fugitive ink (mixture of petroleum jelly and wax) to produce a complicated 3D structure followed by the infusion of epoxy resin already mixed with Grubb's catalyst, which was then cured to obtain a solid network of microchannels. The specimen was tested in a four-point bending system until crack initiation. The crack openings had smaller dimensions (~10 μm) than microchannels (220 μm). Therefore, the healing agent (DCPD) leaks through the microchannels due to the capillary action and it reacts with the Grubb's catalyst present in the epoxy matrix in the crack plane to heal the crack. The specimen was allowed to heal at RT for 12 h and retested for another healing cycle. The data from fracture toughness tests followed by healing cycles showed that healing could be performed up to seven healing cycles. The healing efficiency values varied at every healing cycle with the maximum (70%) at the 2nd cycle and the minimum (~35%) at the 4th cycle.

After a few years, Toohey *et al.*[114] introduced a two-component healing system of epoxy resin and an amine hardener using the same network of microvascular system in the epoxy matrix. It was observed that the number of healing cycles to get a significant recovery increased to 16 cycles with a maximum healing efficiency of ~90% at the 3rd cycle and a minimum of ~30% at the 13th cycle. The possible reason behind the improvement in the number of healing cycles was the self-healing agents. The higher compatibility of the epoxy healing agent with the matrix and the availability of both the reactive components led to increased healing cycles. The Grubb's catalyst in the previous report gets consumed during the healing, and if crack initiates again at the same location, the availability of Grubb's catalyst will be lower for healing the crack. On the other hand, in the case of an epoxy/amine hardener system, both the healing agents were supplied after each healing cycle, thereby increasing the number of cycles of healing for the specimen.

Norris *et al.*[115] prepared a CFRE laminate with a microvascular network to study self-healing using this approach. The micro-vascules of diameter 250 μm were located in the mid-plane of the laminate to provide good connectivity to the damaged area and facilitate the infusion of the healing agent. The microvascular network was filled with epoxy–amine healing agents using micro-syringes. The specimen underwent inter-laminar cracking after the impact and subsequently the healing agents were injected into vascules. The healing was allowed for 7 days at ambient temperature. The damaged specimens were tested for compression after impact (CAI) strength after the healing and a recovery of 97% was observed post healing.

This approach is not feasible in real-life self-healing applications due to the requirement of re-filling of the healing material. This constraint will make it difficult to fulfill self-healing requirements where manual interventions are not possible, *e.g.*, in-service aerospace parts.

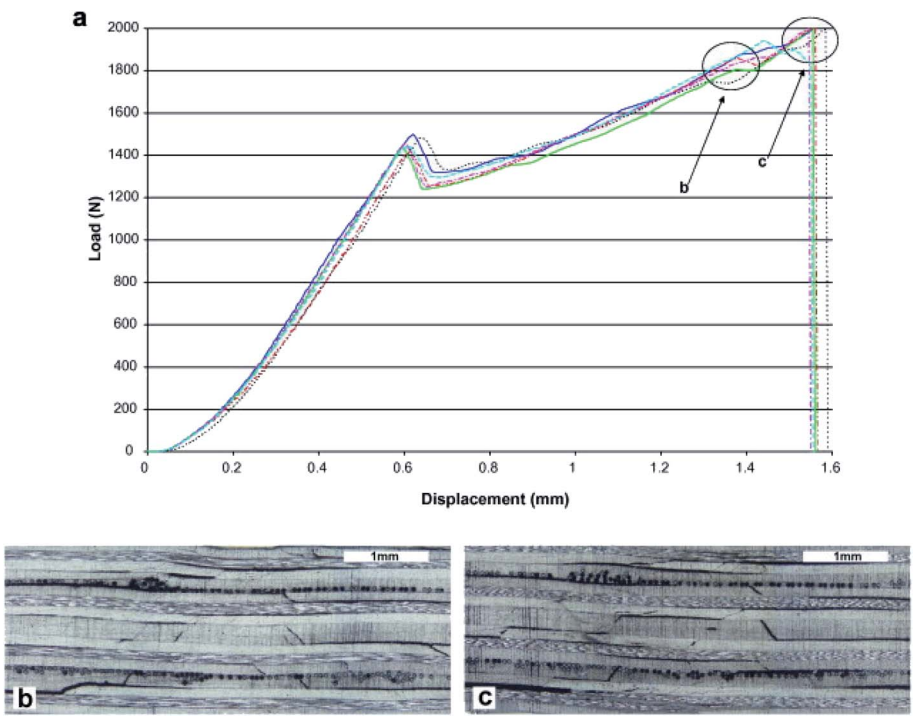

Fig. 14 (a) Typical load–displacement curves for quasi-static indentation of CFRP (3 damaged and 3 healed samples), cross-sectional damage for impact force (b) 1700 N and (c) 2000 N.[116] Reproduced from ref. 116 with permission from Elsevier (2007).

Inspired by the micro-tubular channels and micro-containers of healing agents, Williams *et al.*[116] used hollow glass fibers as containers for healing agents. A CFRE laminate was manufactured with a stacking sequence of $[-45°/90°/45°/0°]_{2s}$ using the hand layup technique. The hollow glass fibers of diameter ~50 μm filled with an epoxy–amine based healing agent were incorporated between 0°/−45° interfaces. The composite specimens were tested by the four-point bending method until crack initiation. The hollow glass fibers got ruptured during the crack propagation thereby releasing the healing agent to the crack. After the damage, the specimens were heated at 125 °C for 75 min to achieve a healing efficiency of ~82%. The corresponding variation in load *vs.* displacement curves are depicted in Fig. 14.

Williams *et al.*[117] also studied self-healing using the CAI test on CFRE laminates. A CFRE laminate was prepared using the hand layup technique with a stacking sequence of $[-45°/90°/45°/0°]_{2s}$. Hollow glass fibers of diameter ~70 μm filled with epoxy–amine healing agents were placed at the interfaces between 0°/−45° plies. After the impact damage the specimens were allowed to heal at 125 °C for 75 min. Post healing, the specimens were tested for compressive strength and a recovery of more than 90% was reported.

Wu *et al.*[118] introduced nano-vascular tubes in the form of nanofibers in CFRE laminates. The disadvantage of micron size containers (microcapsules and hollow glass fibers) is that they act as stress-concentration sites causing early failure of the laminates, and they are not feasible for thin laminate structures. The low nanofiber content (<1 vol%) required to induce self-healing abilities is another advantage over the techniques mentioned above where more than 10 vol% microcapsules were needed. They synthesized nano-fiber mats with fibers having a core–shell morphology by using the co-electrospinning technique. The shell of the nano-fibers was made up of PAN and the core contained the DCPD healing agent. The nanofibers were deposited over CFs and they came in contact with the matrix after the infusion of epoxy resin. The crack initiation at the fiber/matrix interface ruptured the nanofibers and released the healing agent, which reacted with the catalyst present in the matrix and polymerized the DCPD monomer. The CFRE laminates were fabricated using VARTM comprising epoxy/unidirectional fiber mats with a $[0°/\pm45°/90°]_s$ stacking sequence with the epoxy matrix containing a fixed amount of Grubb's catalyst. The nanofiber mats of about 80 μm thickness were deposited at 0°/45° and 45°/90° interfaces because there is a larger probability of interfacial failures along these interfaces. The laminates were subjected to three-point bending tests up to first interlaminar cracking. Followed by a healing cycle of 2 h, the healing efficiency was found to be 97 to 103% measured in terms of flexural stiffness. SEM images provided evidence for the formation of new rough surfaces after the polymerization of healing agents at interfaces. The introduction of nanofiber mats at the interfaces provided a major advantage to target directly at the interfacial healing.

In another report, Neisiany *et al.*[119] used the co-electrospinning technique to produce nanofibers with two different cores, epoxy and amine. PAN was used as the shell material. The nanofibers with two different cores were deposited over unidirectional CF mats. A CFRE laminate was fabricated using VARTM with six layers of unidirectional and parallel aligned CF mats. The healing after three-point bending tests was allowed for 24 h at RT. The healing efficiency of flexural strength ranged from 96–102%. The authors also reported that there was an improvement of 14% in flexural strength after the incorporation of nanofibers into the CFRE laminates. The reason proposed behind this improvement is the Velcro effect provided by the nanofibers. The nanofibers deposited over CFs act as a transverse bridge between the epoxy matrix and CFs thereby strengthening the interface. In line with that, some other researchers manufactured the outer shell of nanofibers from different kinds of polymers. The polypropylene (PP) shell was proposed for better processability. PP nanofibers can be easily deformed and knitted with CFs for complex design applications and their surface can be easily modified to make them compatible with either the matrix or CFs.[120] The PMMA shell was proposed to have advantages of high compatibility with the epoxy matrix and lower strain before breakage.[121]

3.3. Induction of self-healing abilities using the thermo-reversible Diels–Alder (DA) reaction in polymers and CFRE composites

The above discussed approaches for self-healing in CFRE laminates consisted of addition of external self-healing agents and the self-healing ability solely depends on the availability of the incorporated healing agents (catalyst, monomer, epoxy resin and hardener) at the damaged site. Once all the healing agents are consumed, the self-healing ability will cease in the laminate. To overcome this challenge another approach to induce interfacial self-healing ability was introduced. The use of the DA thermo-reversible chemical reaction at the interface of the fibers and matrix will heal the damaged interface by applying heat. The DA thermo-reversible reaction involves the reaction of a diene and a dienophile to form a cyclo-addition compound (DA adduct). The reaction is temperature-controlled and can be reverted to original reactants (retro-DA) by application of a certain temperature.[122,123]

The matrix and the reinforcing fibers were chemically modified to introduce the required reactants for the DA reaction. The modification serves two purposes: (a) introducing the self-healing property with the application of temperature and (b) increasing the interfacial strength between the matrix and fibers by covalent bonding between them thereby improving the mechanical properties of the composite.

Chen *et al.*[124] prepared a cross-linked polymer from bismaleimide (BMI) and furan monomers. The maleimide and furan functional groups react to form a thermo-reversible DA adduct. The resultant T_g of the polymers varied between 30 °C and 80 °C. The polymer was molded into a compact tension specimen with a sharp pre-crack notch and a hole. The hole was created to stop the propagating crack before it breaks the specimen into two pieces in the fracture toughness test. After the failure of the specimen, healing was allowed at 115 °C for 30 min followed by cooling in a chamber at 40 °C for 6 h. The heating at 115 °C was

performed to disconnect the DA adducts following the retro-DA reaction. The cooling operation at 40 °C allowed the DA reaction to form the DA adduct and healed the crack. The average healing efficiency reported was 80% for the first cycle and 78% for the second cycle. Ghezzo *et al.*[125] prepared a CF laminate with a cross-linked polymer of BMI and furan monomers. The polymer melt was infused into unidirectional CF mats $[0°/90°/0°]_s$ using VARTM. Thermo-mechanical studies of the CFRE laminate were performed using a dynamic mechanical spectrometer. The tan δ peak of the CFRE laminate showed that the T_g of the laminate was very close to that of the pure polymer. The dynamic behavior of the composite as a function of temperature showed that as the temperature approached T_g of the polymer matrix (>80 °C), its storage modulus started depleting. These observations suggested that the healing operation should be done at temperatures that do not affect the intrinsic structural properties of the laminate.

Zhang *et al.*[126] performed the DA reaction over CFRE composites by introducing surface maleimide groups over amine-functionalized CFs. The epoxy matrix was functionalized using co-polymerization of the furan group-containing monomer furfuryl glycidyl ether (FGE). IFSS was analyzed by microdroplet single fiber debonding followed by healing of the debonded samples at 90 °C for 1 h and subsequently at RT for 24 h. The authors proposed that during the interfacial damage, the DA adduct preferentially breaks into BMI and furan groups. These groups react to rejoin at a specific temperature as a DA adduct and heal the fiber matrix interface. The results from multiple self-healing cycles showed a decrease in self-healing efficiency as the number of cycles increased. It decreased from 82% for the 1st healing cycle to 58% for the 3rd healing cycle due to uneven breakage of the DA bonds during interfacial failures.

Zhang *et al.*[127] also studied the optimization between IFSS and healing efficiency as a function of %FGE (furan content) in the epoxy matrix of CFRE composites. It was observed that on increasing %FGE, IFSS increased due to the increase in the number of covalent bonds at the interface. On the other hand,

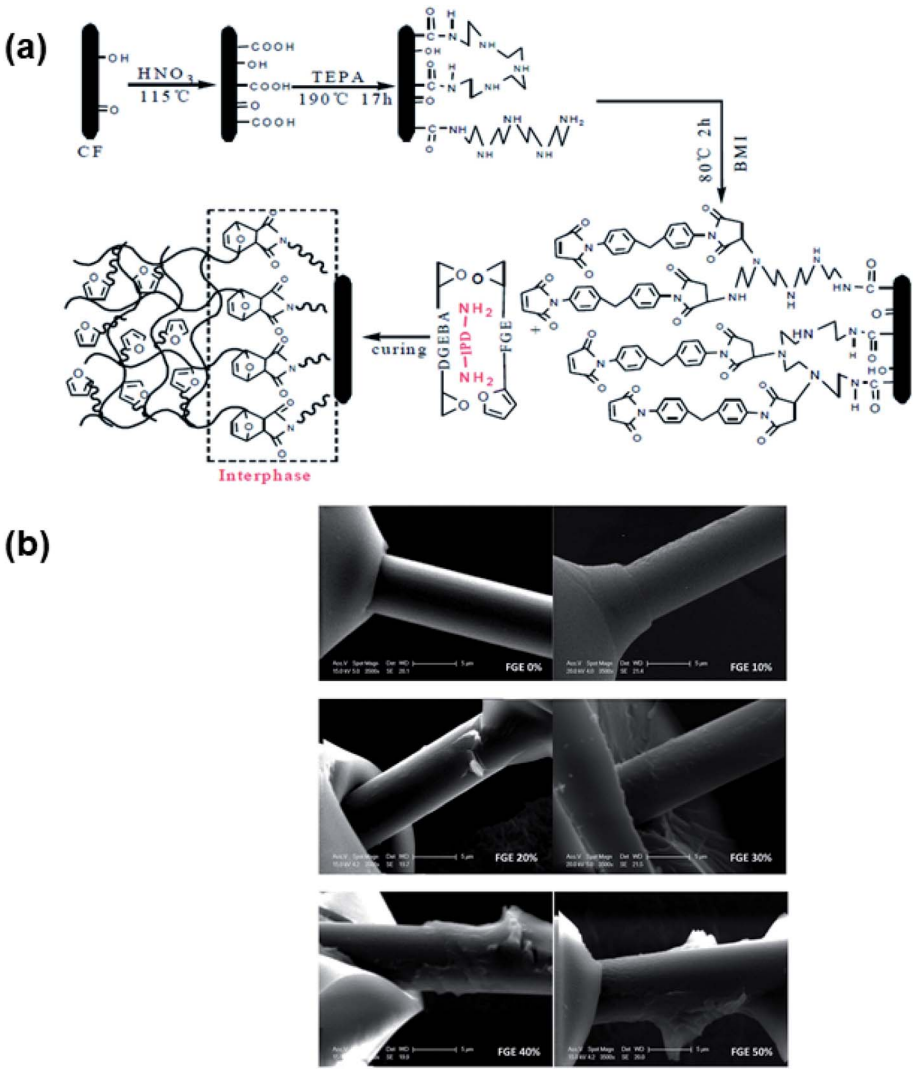

Fig. 15 (a) Formation of a thermo-reversible interphase through fiber and matrix modification. (b) Scanning electron micrographs of fractured epoxy/T700-BMI interfaces after the microdroplet debonding test.[127] Reproduced from ref. 127 with permission from RSC (2016).

a decrease in healing efficiency was observed on increasing % FGE. As the interface of epoxy/CF becomes stronger, the cohesive fracture of the epoxy matrix becomes more dominant (Fig. 15). This reduces the number of free reactant groups at the CF surface to form a DA adduct, which decreases the healing efficiency. The results showed that a trade-off between IFSS and healing efficiency was obtained at 20–30% FGE with 40% healing efficiency. The DA mechanism between BMI and furan groups and the resulting fractured surface morphology of the modified interfaces are shown in Fig. 15.

Kostopoulos *et al.*[128] studied the self-healing of a CFRE modified with BMI resin. The CFRE laminates were prepared by using the vacuum bagging technique. BMI resin was spread between the 11th and 12th layer (mid plane) of the 22-layer unidirectional CF composite. The chosen epoxy matrix already contained furan groups, which reacted with the maleimide group to undergo the DA/retro-DA reaction. The BMI resin impregnated into the other layers during the curing process. The CFRE laminates were cut into a double cantilever beam (DCB) specimen for inter-laminar fracture toughness studies. The specimen was loaded until the crack reached a length of 100 mm. The healing was allowed for 15 min at 130 °C followed by cooling at RT. The authors reported a maximum recovery of 30% in peak load and 23% in fracture energy up to three healing cycles and then a decrease in the next two cycles.

Iacono *et al.*[129] used the epoxy matrix with DA reactants (maleimide and furan functional groups) to induce self-healing ability in a CFRE composite. The composite was manufactured by vacuum bagging using 12 layers of UDs. The specimens were tested for ILSS and shear mode II end notch failure (ENF). To perform the ENF test, a polyimide film (Kapton layer) was incorporated in the mid-plane to facilitate the initial delamination, which leads to mutual sliding of separated parts. Two healing cycles were performed after damage, healing at 120 °C

Table 6 A summary of self-healing studies in CFRE using different approaches

Sl no.	Healing agent	Healing cycle	Mechanical properties/tests	% Recovery	Ref.
1	UF microcapsules containing DCPD	48 h at RT	WTCB interlaminar fracture test (max. Critical load)	38%	111
2	UF microcapsules containing DCPD	24 h at RT followed by 24 h at 80 °C	Tensile testing (transverse direction)	19%	112
3	Rechargeable microvascular network containing epoxy–amine healing agent	7 days at RT	CAI	~97%	115
4	Hollow glass fibers containing epoxy–amine healing agent	125 °C for 75 min	Four-point bending	~82%	116
5	Hollow glass fibers containing epoxy–amine healing agent	125 °C for 75 min	CAI	>90%	117
6	Core–shell nanofibers Core: DCPD Shell: PAN	2 h at RT	Flexural stiffness	97 to 103%	118
7	Two types of core–shell nanofibers Core: epoxy and amine Shell: PAN	24 h at RT	Flexural stiffness	96 to 102%	119
8	Maleimide functionalized CFs and FGE functionalised epoxy (DA reaction)	90 °C for 1 h and RT for 24 h.	IFSS (microdroplet debonding test)	82% (max.)	126
9	Maleimide functionalized CFs and FGE functionalised epoxy (DA reaction)	90 °C for 1 h and RT for 24 h.	IFSS (microdroplet debonding test)	~40%	127
10	BMI incorporated between mid-layers of CFRE laminates	130 °C for 15 min and cooling to RT	Inter-laminar fracture toughness	23%	128
11	Epoxy matrix having DA reactants	120 °C for 20 min 90 °C for 12 h	ILSS Fracture toughness	95.1% (1st cycle) 81.7% (2nd cycle) 89.7% (1st cycle) 52.4% (2nd cycle)	129
12	BMI incorporated between mid-layers of CFRE laminates	150 °C for 5 min and cooling to RT	Fatigue behaviour (tension–tension mode)	~75%	130
13	BMI covalently deposited on the CF surface, GO dispersed in the epoxy matrix	60 °C for 24 h, slow-cooling to RT	ILSS	~70%	131

for 20 min and at 90 °C for 12 h. The ILSS test exhibited the recovery of 95.1% and 81.7%, and fracture toughness in the ENF test exhibited the recovery of 89.7% and 52.4%, in the first and second healing cycles, respectively.

In a recent research study, Kostopoulos *et al.*[130] also studied fatigue behavior improvement with the same composite system mentioned in ref. 128. The CFRE composite was prepared by vacuum bagging having 16 plies with the stacking sequence $[45°/-45°/0°/90°]_{2S}$. BMI resin was introduced at the interface of $-45°$ and 0° plies, and has high stiffness mismatch. The specimens were cut in the shape of open hole tensile specimens. The hole leads to stress concentration and reduces the net section in the specimen during testing. It also resembles the notched design in aerospace parts (*e.g.* fastener holes). The specimens were subjected to a maximum stress of $0.8 \times \sigma_{UTS}$ with $R = 0.1$ at a frequency of 5 Hz in the tension–tension mode. The healing and retesting were performed after every 10 000 cycles. The healing was allowed for 5 min at 150 °C followed by cooling to RT. The results showed that there was an improvement of 75% in the fatigue life of the specimen compared to the control sample (without BMI).

Recent work by Banerjee *et al.*[131] focused on designing a protocol for modified CFRP laminates with improved mechanical strength properties as well as self-healing behavior through modifications on both the bulk epoxy matrix and carbon fiber surface. A Diels'–Alder (D–A) reaction with GO dispersed in epoxy and BMI covalently coated over the carbon fiber surface led to increased flexural strength and ILSS by 30% and 47%, respectively. After a self-healing cycle triggered at 60 °C, they exhibited a recovery in their ILSS values up to 70%. Their work reflected that facile methods provided not only CFRPs with improved strengths but also a certain degree of restoration of original mechanical properties using simple triggers such as heat and/or pressure.

Self-healing has revolutionised the world of materials science by substantially extending the life-cycle of materials. However, for systems such as CFRE laminates, achievement of recovery of mechanical properties to their original level is a challenging idea. Since mechanical behaviour of anisotropic non-homogeneous systems such as CFRE laminates largely depends on the weaker region of the fabricated component, the direction of failure in such systems is in most cases unpredictable. While microcapsules to a certain extent succeeded in mimicking biological systems, they in turn deteriorated the original mechanical properties because of the introduction of several interfacial regions that acted as potential stress-concentrators. Furthermore, while intrinsic self-healable reactions such as DA may promise restoration of debonded regions in the scale of atomic chains, propagating microcracks remain unattended by such thermo-reversible bonds. Therefore, the field of mechanical self-healing of CFRE laminates is wide open to research, and the introduction of technology that could synergistically improve the original mechanical properties and promote restoration of weak debonded interfacial sites as well as bulk microcrack healing is awaited.

A summary of the above results is presented in Table 6.

4. Discussions and conclusion

Although sizing was the first major modification route for the interface that generated promising results for mechanical properties, several studies disapproved a positive correlation between sizing and mechanical properties. While Harris *et al.*[31] indicated no significant correlation between sizing and visco-elastic properties of CFREs, Park *et al.*[132] revealed a deteriorating effect of sizing on the fibers' ductility and crack absorbing power. Dai *et al.*[133] further established a correlation between the thickness of sizing and IFSS properties. However, novel routes of developing sizing agents that provided better compatibility with the fiber and matrix were established over the years.[34–36] Nevertheless, while sizing was observed to promote better interfacial properties in several cases, incompatibility with the risk of forming a third phase limited its success.

Modification of the epoxy matrix was started as early as in 1987 with studies such as that of Andrew Garton,[37] which was then followed by similar protocols over the years. While clay[38,39] was used originally as the filler, the rise of graphene-based derivatives shifted the modifiers to carbonaceous nanoparticles, such as CNTs, CFs, GNPs, NCAs[47–51] *etc.* Furthermore, 3D structures[54] with carbon based foams or nanodiamonds too were explored. In all these cases, the incorporation of carbon based derivatives not only formed a solution compatible with the matrix, but the presence of a π–π interaction with the fibers allowed the modified matrix to better adhere to the fibers and form a stronger interface. However, although the interface specific mechanical properties such as IFSS and ILSS showed some improvements alongside other properties such as flexural strength, impact strength and fracture toughness, problems involving improper deposition after a minimal loading rate and the reduced possibility of most nanoparticles interacting at the interface instead of being submerged in the bulk of the matrix persisted.

In order to ensure higher interaction at the interface, deposition or growth of nanoparticles directly on the surface of the fibers proved to be more effective, although it is a risky operation prone to deteriorating the fiber integrity. The initial routes were those of oxidative surface treatments on the fibers resulting in improved interface-related mechanical properties such as ILSS and IFSS.[57,70] However, chances of decrease in the content of activated carbon and polar surface energy upon over-optimization of time/temperature of heat treatment, as observed by Dai *et al.*,[59] followed by generation of pits on the fiber surface limited the harsh treatments such as fiber oxidation. So, the research shifted to non-oxidative surface treatments such as polymeric functionalization.

Polymeric functionalization involved synthesizing or polymerizing a monomer[79–81,86] or grafting polymers directly over the fibers.[82–84] In the same way, carbonaceous nanoparticles were either deposited or grown over carbon fibers. While Dong *et al.*[87] and Yao *et al.*[90] grew CB and CNT particles using chemical vapour deposition, Batista *et al.*[88] and Zhang *et al.*[93] incorporated CNCs and GO into the sizing agent and CFs were dipped in the sizing solution. A significant interfacial improvement in all the cases was observed reflecting the enhancement of IFSS

and ILSS properties. Functionalization of the nanoparticles prior to their integration into the fibers further enhanced uniform deposition and enhanced the properties. A higher surface roughness and surface energy inducing better adhesion of epoxy led to a stronger interface region transferring the stress more effectively. However, in terms of cost effectiveness of the method of nanoparticle deposition, metals and metal oxides of Fe, Cu and Ti have proven to be better choices than carbonaceous nanoparticles. While major improvements have been observed for TiO_2-based nanostructures deposited over carbon fibers,[99–101] Fakhrhoseini *et al.*[101] successfully deposited nano-magnetite on fibers. Since nano-metals in itself lack chemical interactions with the epoxy matrix, combining them with carbonaceous particles[96,97] witnessed a greater effect on the resulting properties.

Over the years, the vast use of CFREs has given rise to a wide variety of research that deals with tackling the interface of such non-homogeneous structures to provide improved mechanical properties. However, while there has been a substantial development from the initial days of sizing to electrodeposition techniques of depositing nanoparticles over fibers, several lacunae still exist in each of the techniques mentioned necessitating the development of an optimized fabrication technique.

With the advent of self-healing in epoxy composites, the idea of a remedying technology for CFREs has taken birth. While the use of microcapsules in CFREs was relatively easy in terms of synthesis and mixing which provided a healing efficiency of ~38%,[111] it had some disadvantages of non-repeatability of healing and increasing viscosity of the epoxy resin during fabrication. Next came the microvascular network made of waxes and hollow glass fibers providing a healing efficiency of ~97% with the possibility of recharging healing agents after every damage cycle.[115] However, the micro-sized tubes acted as defects resulting in deterioration of a near-net fabrication for thin lamina systems. Core–shell nano-fibers came into picture with an epoxy/amine core and PAN as the shell material. The fibers were synthesized using the electrospinning technique. A healing efficiency of more than 100% was achieved with such nano-fibers.[118] The use of nanofibers led to the Velcro type effect between the epoxy and carbon fibers leading to improvement in the intrinsic properties of laminates. While the above methods dealt with an extrinsic form of self-healing, the incorporation of DA reaction moieties in CFREs induced thermoreversible healing properties in the laminates providing an intrinsic form of self-healing. This self-healing worked differently in comparison to the previous ones as the de-bonded or de-laminated sites were more focused in this form of self-healing as opposed to crack refilling. The use of DA adducts provided a maximum healing efficiency of ~95% in the first healing cycle.[129] Furthermore, multiple healing cycles were achieved due to rDA and DA reactions leading to temperature controlled healing properties in CFRE laminates.

5. Outlook and perspective

With the advent of CFRE composites around 50 years ago in the aerospace industry, interfacial tuning has been seen as a major area of research to combat failure in aircraft parts and increase the aircraft's service life. The major mode of improving interfacial strength involves increasing the CF's surface area and allowing better wettability of the fibers. This article primarily focused on various techniques used for modifying both the epoxy matrix and the CFs. Any chemical modification of the CFs, while enhancing the interfacial strength and toughness, damages the fibers and decreases fiber strength. Therefore, an optimized surface modification becomes necessary to cover the fiber defect sites. Furthermore, two major challenges pertaining to CFRPs that include high temperature application and interfacial rebonding at the cost of pristine mechanical properties are still being researched on. While a gradient interface that develops good adhesion on both the fibers and the matrix, and a thermal expansion coefficient that lies midway to the two components are a need of the hour, it must also be ensured that the interface formed does not lead to creation of further weak sites that deteriorate the original mechanical properties. Several new technologies are being developed in this area. Metal–organic-frameworks (MOFs) are a class of fascinating crystalline materials with extremely high surface areas and reactive sites. Li *et al.*[134] grew a photo switchable MOF film over CFs through a layer-by-layer approach. They observed better interface adhesion with the application of MOFs. Additionally, MOFs as nano carriers have the potential to heal a failed interface.

The prospect of modifying the interface with surface treatments and nanoparticles stems from the extremely high surface area, which enhances both the polar component and the dispersive component of the surface energy. Thus, certain nanoparticles with hyper branched structures or larger surface areas have been synthesized in recent times to modify the interface region. In order to incorporate nanoparticles with a high degree of functional groups, Shen *et al.*[135] prepared CF/CNT/OA-POSS reinforcement by grafting CNTs and octa-aminopropyl polyhedral oligomeric silsesquioxane (OA-POSS) onto CF surfaces to improve the mechanical properties and interfacial performance. The octahedral structure of POSS can change the interface toughness modulus and interfacial strength between the reinforced fibers and resin.

MXenes[136,137] are upcoming new age materials with a wide range of potential applications because of their high surface activity and energy storage capability. Exploiting the vast scope of MXenes, Liu *et al.*[138] recently worked on functionalizing CFs with MXenes (Ti_3C_2). MXenes have a strong polarity that makes them adhere extensively with acid-functionalized CFs. At the same time, they form a chemical bridge with the epoxy matrix and enhance its wettability with the fibers. Their work was quite promising in potentially enhancing the mechanical properties between CFs and epoxy by forming a strong interfacial connection between CFs and epoxy resin.

In recent times, the concept of self-healable parts in aircraft components is gaining wide attention. However, there has not been much research on the lines of a synergistic improvement in laminates' interfacial properties that can induce self-healability in the structure. This results from the dearth of the feasibility of surface modification of CFs without hampering their original mechanical properties. Therefore, the scope of research on CFRE laminates with agents having self-healable

interfaces, which will in turn reduce the prospects of complete replacement of a component on failure, higher service life and cost-effectiveness lies open.

Abbreviations

AA	Acrylic acid
APTES	Aminopropyl triethoxysilane
AFM	Atomic force microscopy
APO	Atmospheric plasma oxidation
BMI	Bismaleimide
BNNP	Boron nitride nanoparticles
CA	Carbon aerogel
CB	Carbon black
CF	Carbon fibre
CFRE	Carbon fiber reinforced epoxy
CFRP	Carbon fibre reinforced polymer
CNC	Carbon-nanocrystal
CNT	Carbon nanotube
CAI	Compression after impact
TCT	Cyanuric chloride
DAAM	Diacetone acrylamide
DCPD	Dicyclopentadiene
DA	Diels–Alder
DETA	Diethylenetriamine
DSC	Differential scanning calorimetry
DCB	Double cantilever beam
DMTA	Dynamic mechanical thermal analysis
EPD	Electrophoretic deposition
EP	Epoxy
ENF	End notch failure
EG	Expanded graphite
FRP	Fiber-reinforced polymer
FTIR	Fourier transform infrared spectroscopy
FGE	Furfuryl glycidyl ether
GNP	Graphene nanoplatelets
GO	Graphene oxide
HMTA	Hexamethylene tetra-amine
HCFRP	Hybrid carbon fiber reinforced polymer
HPEEK	Hydroxylated poly(ether ether ketone)
HTHBP	Hydroxyl-terminated hyperbranched polymer
HBPU	Hyperbranched polyurethane
IR	Infrared spectroscopy
ILSS	Inter laminar shear strength:
IL	Ionic liquid
IPDI	Isophorone diisocyanate
MAH-*g*-PP	Maleic anhydride grafted polypropylene
MOF	Metal–organic-framework
MB	Methylene blue
MDI	Methylene diphenyl isocyanate
MWCNT	Multiwall carbon nanotube
NCA	Nano carbon aerogels
NCP	Nano carbon particles
NR	Nanorods
NW	Nanowires
NDT	Non-destructive tests
NF	Nylon nanofibers
OA-POSS	Octa-aminopropyl polyhedral oligomeric silsesquioxane
PAN	Polyacrylonitrile
PBZ	Polybenzoxazine
PZSNT	Poly(cyclotriphosphazene-*co*-4,4′-sulfonyldiphonel) nanotube
PDA	Polydopamine
PEI	Poly ether imine
PMMA	Poly-methyl-methacrylate
PTFE	Polytetrafluoroethylene
ROMP	Ring-opening metathesis polymerization
SEM	Scanning electron microscopy
SCF	Sized carbon fibers
SIL	Solvate ionic liquid
TDCB	Tapered double cantilever beam
TETA	Tetraethylene tetra-amine
TEM	Transmission electron microscopy
TEPA	Tetraethylenepentamine
TOAM	Tris(hydroxymethyl)aminomethane
UF US	Unfunctionalized unsized
UD	Unidirectional
UF	Urea-formaldehyde
VARTM	Vacuum assisted resin transfer moulding
WTCB	Width tapered cantilever beam

Conflicts of interest

There are no conflicts to declare.

References

1 J. Schultz, L. Lavielle and C. Martin, The role of the interface in carbon fibre-epoxy composites, *J. Adhes.*, 1987, **23**(1), 45–60.
2 M. A. Meyers and K. K. Chawla, *Mechanical Behavior of Materials*, Cambridge University Press, 2008.
3 K. K. Chawla, *Composite Materials: Science and Engineering*, Springer Science & Business Media, 2012.
4 M. Mrazova, Advanced composite materials of the future in aerospace industry, *Incas. Bull*, 2013, **5**(3), 139.
5 J. Hughes, The carbon fibre/epoxy interface—a review, *Compos. Sci. Technol.*, 1991, **41**(1), 13–45.
6 D. Hull, *Materiales Compuestos*, Reverté, 1987.
7 K. K. Chawla, *Fibrous Materials*, Cambridge University Press, 1998.
8 L. Drzal and M. Madhukar, Fibre-matrix adhesion and its relationship to composite mechanical properties, *J. Mater. Sci.*, 1993, **28**(3), 569–610.
9 S. Kasahara, J. Koyanagi, K. Mori and M. Yabe, Evaluation of interface properties of carbon fiber/resin using the full atomistic model considering the electric charge state, *Adv. Compos. Mater.*, 2020, **30**(2), 164–175.
10 Z. Liu, B. Ren, H. Ding, H. He, H. Deng, C. Zhao, P. Wang and D. D. Dionysiou, Simultaneous regeneration of cathodic activated carbon fiber and mineralization of desorbed contaminations by electro-peroxydisulfate

process: Advantages and limitations, *Water Res.*, 2020, **171**, 115456.
11 Y. Altin, H. Yilmaz, O. F. Unsal and A. C. Bedeloglu, Graphene oxide modified carbon fiber reinforced epoxy composites, *J. Polym. Eng.*, 2020, **40**(5), 415–420.
12 P. E. Lopes, D. Moura, L. Hilliou, B. Krause, P. PÃtschke, H. Figueiredo, R. Alves, E. Lepleux, L. Pacheco and M. C. Paiva, Mixed carbon nanomaterial/epoxy resin for electrically conductive adhesives, *J. Compos. Sci.*, 2020, **4**(3), 105.
13 M. C. Andrews, R. J. Day, X. Hu and R. J. Young, Deformation micromechanics in high-modulus fibres and composites, *Compos. Sci. Technol.*, 1993, **48**(1–4), 255–261.
14 Y. Huang and R. J. Young, Interfacial micromechanics in thermoplastic and thermosetting matrix carbon fibre composites, *Composites, Part A*, 1996, **27**(10), 973–980.
15 S.-Y. Fu, X.-Q. Feng, B. Lauke and Y.-W. Mai, Effects of particle size, particle/matrix interface adhesion and particle loading on mechanical properties of particulate polymer composites, *Composites, Part B*, 2008, **39**(6), 933–961.
16 L. Jin, L. Liu, J. Fu, C. Fan, M. Zhang, M. Li and Y. Ao, Three-dimensional Interconnected Nanosheet Architecture as a Transition Layer and Nanocontainer for Interfacial Enhancement of Carbon Fiber/Epoxy Composites, *Ind. Eng. Chem. Res.*, 2019, **58**(47), 21441–21451.
17 S. Thomas, D. Rouxel and D. Ponnamma, *Spectroscopy of polymer nanocomposites*, William Andrew Publishing, Amsterdam, 2016.
18 R. Diefendorf, Comparison of the Various New High Modulus Fibers for Reinforcement of Advanced Composites with Polymers, Metals and Ceramics as Matrix, in *Carbon Fibres and Their Composites*, Springer, 1985, pp. 46–61.
19 H. Puliyalil and U. Cvelbar, Selective plasma etching of polymeric substrates for advanced applications, *Nanomaterials*, 2016, **6**(6), 108.
20 K. R. Reddy, A. El-Zein, D. W. Airey, F. Alonso-Marroquin, P. Schubel and A. Manalo, Self-healing polymers: Synthesis methods and applications, *Nano-Struct. Nano-Objects*, 2020, **23**, 100500.
21 H. Pulikkalparambil, S. Siengchin and J. Parameswaranpillai, Corrosion protective self-healing epoxy resin coatings based on inhibitor and polymeric healing agents encapsulated in organic and inorganic micro and nanocontainers, *Nano-Struct. Nano-Objects*, 2018, **16**, 381–395.
22 B. D. S. Deeraj, R. Harikrishnan, J. S. Jayan, A. Saritha and K. Joseph, Enhanced visco-elastic and rheological behavior of epoxy composites reinforced with polyimide nanofiber, *Nano-Struct. Nano-Objects*, 2020, **21**, 100421.
23 S. Thomas and A. Surendran, *Self-Healing Polymer-Based Systems*, Elsevier, 2020.
24 S. R. White, N. Sottos, P. Geubelle, J. Moore, M. R. Kessler, S. Sriram, E. Brown and S. Viswanathan, Autonomic healing of polymer composites, *Nat. Commun.*, 2001, **409**(6822), 794.
25 W. Zhang, J. Duchet and J. Gérard, Effect of epoxy matrix architecture on the self-healing ability of thermo-reversible interfaces based on Diels–Alder reactions: demonstration on a carbon fiber/epoxy microcomposite, *RSC Adv.*, 2016, **6**(115), 114235–114243.
26 J. Schultz and M. Nardin, Some physico-chemical aspects of the fibre-matrix interphase in composite materials, *J. Adhes.*, 1994, **45**(1–4), 59–71.
27 L. G. Tang and J. L. Kardos, A review of methods for improving the interfacial adhesion between carbon fiber and polymer matrix, *Polym. Compos.*, 1997, **18**(1), 100–113.
28 S. Jenkins, G. Emmerson, P. McGrail and R. Robinson, Thermoplastic sizing of carbon fibres in high temperature polyimide composites, *J. Adhes.*, 1994, **45**(1–4), 15–27.
29 D. M. Blackketter, D. Upadhyaya, T. R. King and J. A. King, Evaluation of fiber surfaces treatment and sizing on the shear and transverse tensile strengths of carbon fiber-reinforced thermoset and thermoplastic matrix composites, *Polym. Compos.*, 1993, **14**(5), 430–436.
30 J. Lesko, R. Swain, J. Cartwright, J. Chin, K. Reifsnider, D. Dillard and J. Wightman, Interphases developed from fiber sizings and their chemical-structural relationship to composite compressive performance, *J. Adhes.*, 1994, **45**(1–4), 43–57.
31 B. Harris, O. Braddell, D. Almond, C. Lefebvre and J. Verbist, Study of carbon fibre surface treatments by dynamic mechanical analysis, *J. Mater. Sci.*, 1993, **28**(12), 3353–3366.
32 S.-J. Park and J.-R. Lee, Bending fracture and acoustic emission studies on carbon–carbon composites: effect of sizing treatment on carbon fibres, *J. Mater. Sci.*, 1998, **33**(3), 647–651.
33 Z. Dai, F. Shi, B. Zhang, M. Li and Z. Zhang, Effect of sizing on carbon fiber surface properties and fibers/epoxy interfacial adhesion, *Appl. Surf. Sci.*, 2011, **257**(15), 6980–6985.
34 D. J. Eyckens, L. Servinis, C. Scheffler, E. Wölfel, B. Demir, T. R. Walsh and L. C. Henderson, Synergistic interfacial effects of ionic liquids as sizing agents and surface modified carbon fibers, *J. Mater. Chem. A*, 2018, **6**(10), 4504–4514.
35 X. Yuan, B. Zhu, X. Cai, J. Liu, K. Qiao and J. Yu, Optimization of interfacial properties of carbon fiber/epoxy composites *via* a modified polyacrylate emulsion sizing, *Appl. Surf. Sci.*, 2017, **401**, 414–423.
36 K. M. Beggs, L. Servinis, T. R. Gengenbach, M. G. Huson, B. L. Fox and L. C. Henderson, A systematic study of carbon fibre surface grafting *via in situ* diazonium generation for improved interfacial shear strength in epoxy matrix composites, *Compos. Sci. Technol.*, 2015, **118**, 31–38.
37 A. Garton, W. T. Stevenson and S. Wang, Interfacial reactions in carbon—epoxy composites, *Br. Polym. J.*, 1987, **19**(5), 459–467.
38 Y. Xu and S. Van Hoa, Mechanical properties of carbon fiber reinforced epoxy/clay nanocomposites, *Compos. Sci. Technol.*, 2008, **68**(3–4), 854–861.

39 R. Oliwa, M. Heneczkowski, J. Oliwa and M. Oleksy, Mechanical strength of epoxy/organoclay/carbon fiber hybrid composites, *Polym. J.*, 2017, **62**, 658–665.
40 F. H. Gojny, J. Nastalczyk, Z. Roslaniec and K. Schulte, Surface modified multi-walled carbon nanotubes in CNT/epoxy-composites, *Chem. Phys. Lett.*, 2003, **370**(5–6), 820–824.
41 J. A. Kim, D. G. Seong, T. J. Kang and J. R. Youn, Effects of surface modification on rheological and mechanical properties of CNT/epoxy composites, *Carbon*, 2006, **44**(10), 1898–1905.
42 A. Godara, L. Mezzo, F. Luizi, A. Warrier, S. V. Lomov, A. W. Van Vuure, L. Gorbatikh, P. Moldenaers and I. Verpoest, Influence of carbon nanotube reinforcement on the processing and the mechanical behaviour of carbon fiber/epoxy composites, *Carbon*, 2009, **47**(12), 2914–2923.
43 Y. Zhou, F. Pervin, L. Lewis and S. Jeelani, Fabrication and characterization of carbon/epoxy composites mixed with multi-walled carbon nanotubes, *Mater. Sci. Eng., A*, 2008, **475**(1–2), 157–165.
44 I. Zaman, T. T. Phan, H.-C. Kuan, Q. Meng, L. T. B. La, L. Luong, O. Youssf and J. Ma, Epoxy/graphene platelets nanocomposites with two levels of interface strength, *Polymer*, 2011, **52**(7), 1603–1611.
45 E. Kandare, A. A. Khatibi, S. Yoo, R. Wang, J. Ma, P. Olivier, N. Gleizes and C. H. Wang, Improving the through-thickness thermal and electrical conductivity of carbon fibre/epoxy laminates by exploiting synergy between graphene and silver nano-inclusions, *Composites, Part A*, 2015, **69**, 72–82.
46 C. Y. Lee, J.-H. Bae, T.-Y. Kim, S.-H. Chang and S. Y. Kim, Using silane-functionalized graphene oxides for enhancing the interfacial bonding strength of carbon/epoxy composites, *Composites, Part A*, 2015, **75**, 11–17.
47 A. K. Pathak, M. Borah, A. Gupta, T. Yokozeki and S. R. Dhakate, Improved mechanical properties of carbon fiber/graphene oxide-epoxy hybrid composites, *Compos. Sci. Technol.*, 2016, **135**, 28–38.
48 Y.-C. Chiou, H.-Y. Chou and M.-Y. Shen, Effects of adding graphene nanoplatelets and nanocarbon aerogels to epoxy resins and their carbon fiber composites, *Mater. Des.*, 2019, **178**, 107869.
49 M. Kim, K. Rhee, J. Lee, D. Hui and A. K. Lau, Property enhancement of a carbon fiber/epoxy composite by using carbon nanotubes, *Composites, Part B*, 2011, **42**(5), 1257–1261.
50 T. Y. Chou, H.-Y. Tsai and M. C. Yip, Preparation of CFRP with modified MWCNT to improve the mechanical properties and torsional fatigue of epoxy/polybenzoxazine copolymer, *Composites, Part A*, 2019, **118**, 30–40.
51 D. Quan, J. L. Urdániz and A. Ivanković, Enhancing mode-I and mode-II fracture toughness of epoxy and carbon fibre reinforced epoxy composites using multi-walled carbon nanotubes, *Mater. Des.*, 2018, **143**, 81–92.
52 M. Hussain, A. Nakahira and K. Niihara, Mechanical property improvement of carbon fiber reinforced epoxy composites by Al2O3 filler dispersion, *Mater. Lett.*, 1996, **26**(3), 185–191.
53 H. Ulus, Ö. S. Şahin and A. Avcı, Enhancement of flexural and shear properties of carbon fiber/epoxy hybrid nanocomposites by boron nitride nano particles and carbon nano tube modification, *Fibers Polym.*, 2015, **16**(12), 2627–2635.
54 A. Bisht, K. Dasgupta and D. Lahiri, Investigating the role of 3D network of carbon nanofillers in improving the mechanical properties of carbon fiber epoxy laminated composite, *Composites, Part A*, 2019, **126**, 105601.
55 P. Katti, K. V. Kundan, S. Kumar and S. Bose, Poly(ether ether ketone)-Grafted Graphene Oxide Interconnects Enhance Mechanical, Dynamic Mechanical, and Flame-Retardant Properties in Epoxy Laminates, *ACS Omega*, 2018, **3**(12), 17487–17495.
56 J. Zhang, *Different Surface Treatments of Carbon Fibers and Their Influence on the Interfacial Properties of Carbon Fiber/epoxy Composites*, 2012.
57 J. W. Herrick, P. E. Gruber Jr and F. T. Mansur, *Surface Treatments for Fibrous Carbon Reinforcements; Avco Missiles Space and Electronics Group Lowell Ma Avco Space Systems Div*, 1966.
58 D. Scola and M. Basche, Treatment of carbon fibers, US3772429A, 1973.
59 Z. Dai, B. Zhang, F. Shi, M. Li, Z. Zhang and Y. Gu, Effect of heat treatment on carbon fiber surface properties and fibers/epoxy interfacial adhesion, *Appl. Surf. Sci.*, 2011, **257**(20), 8457–8461.
60 M. Morra, E. Occhiello, F. Garbassi and L. Nicolais, Surface studies on untreated and plasma-treated carbon fibers, *Compos. Sci. Technol.*, 1991, **42**(4), 361–372.
61 P. Commercon and J. Wightman, Surface characterization of plasma treated carbon fibers and adhesion to a thermoplastic polymer, *J. Adhes.*, 1992, **38**(1–2), 55–78.
62 L. Yuan, C. Chen, S. Shyu and J. Lai, Plasma surface treatment on carbon fibers. Part 1: Morphology and surface analysis of plasma etched fibers, *Compos. Sci. Technol.*, 1992, **45**(1), 1–7.
63 L. Yuan, S. Shyu and J. Lai, Plasma surface treatments of carbon fibers. Part 2: Interfacial adhesion with poly(phenylene sulfide), *Compos. Sci. Technol.*, 1992, **45**(1), 9–16.
64 R. E. Allred and W. C. Schimpf, CO_2 plasma modification of high-modulus carbon fibers and their adhesion to epoxy resins, *J. Adhes. Sci. Technol.*, 1994, **8**(4), 383–394.
65 N. Dilsiz, E. Ebert, W. Weisweiler and G. Akovali, Effect of plasma polymerization on carbon fibers used for fiber/epoxy composites, *J. Colloid Interface Sci.*, 1995, **170**(1), 241–248.
66 N. P. Vaidyanathan, V. N. Kabadi, R. Vaidyanathan and R. L. Sadler, Surface treatment of carbon fibers using low temperature plasma, *J. Adhes.*, 1995, **48**(1–4), 1–24.
67 N. Chand, E. Schulz and G. Hinrichsen, Adhesion improvement of carbon fibres by plasma treatment and evaluation by pull-out, *J. Mater. Sci. Lett.*, 1996, **15**(15), 1374–1375.

68 G. Bogoeva-Gaceva, E. Mäder, L. Haüssler and A. Dekanski, Characterization of the surface and interphase of plasma-treated HM carbon fibres, *Composites, Part A*, 1997, **28**(5), 445–452.

69 C. Pittman Jr, W. Jiang, G.-R. He and S. Gardner, Oxygen plasma and isobutylene plasma treatments of carbon fibers: determination of surface functionality and effects on composite properties, *Carbon*, 1998, **36**(1–2), 25–37.

70 S. Erden, K. K. Ho, S. Lamoriniere, A. F. Lee, H. Yildiz and A. Bismarck, Continuous atmospheric plasma oxidation of carbon fibres: influence on the fibre surface and bulk properties and adhesion to polyamide 12, *Plasma Chem. Plasma Process.*, 2010, **30**(4), 471–487.

71 J.-K. Kim and Y.-W. Mai, *Engineered Interfaces in Fiber Reinforced Composites*, Elsevier, 1998.

72 S. Yumitori and Y. Nakanishi, Effect of anodic oxidation of coal tar pitch-based carbon fibre on adhesion in epoxy matrix: Part 1. Comparison between H_2SO_4 and NaOH solutions, *Composites, Part A*, 1996, **27**(11), 1051–1058.

73 A. Fukunaga and S. Ueda, Anodic surface oxidation for pitch-based carbon fibers and the interfacial bond strengths in epoxy matrices, *Compos. Sci. Technol.*, 2000, **60**(2), 249–254.

74 P. Morgan, *Carbon Fibers and Their Composites*, CRC Press, 2005.

75 J. Goan and S. Prosen, *Interfacial Bonding in Graphite Fiber-Resin Composites (Graphite Fiber-Epoxy Resin Composites Interfacial Bonding, Describing Various Surface Treatments for Increased Interlaminar Shear Strength)*, 1969.

76 J. Donnet and G. Guilpain, Surface characterization of carbon fibres, *Composites*, 1991, **22**(1), 59–62.

77 G. Dagli and N. H. Sung, Properties of carbon/graphite fibers modified by plasma polymerization, *Polym. Compos.*, 1989, **10**(2), 109–116.

78 C. Pittman Jr, G.-R. He, B. Wu and S. Gardner, Chemical modification of carbon fiber surfaces by nitric acid oxidation followed by reaction with tetraethylenepentamine, *Carbon*, 1997, **35**(3), 317–331.

79 Z. Wen, X. Qian, Y. Zhang, X. Wang, W. Wang and S. Song, Electrochemical polymerization of carbon fibers and its effect on the interfacial properties of carbon reinforced epoxy resin composites, *Composites, Part A*, 2019, **119**, 21–29.

80 L. Shi, L. Ma, P. Li, M. Wang, S. Guo, P. Han and G. Song, The effect of self-synthesized hydroxyl-terminated hyperbranched polymer interface layer on the properties of carbon fiber reinforced epoxy composites, *Appl. Surf. Sci.*, 2019, **479**, 334–343.

81 M. Andideh and M. Esfandeh, Effect of surface modification of electrochemically oxidized carbon fibers by grafting hydroxyl and amine functionalized hyperbranched polyurethanes on interlaminar shear strength of epoxy composites, *Carbon*, 2017, **123**, 233–242.

82 M. Zhao, L. Meng, L. Ma, G. Wu, Y. Wang, F. Xie and Y. Huang, Interfacially reinforced carbon fiber/epoxy composites by grafting melamine onto carbon fibers in supercritical methanol, *RSC Adv.*, 2016, **6**(35), 29654–29662.

83 M. T. Aljarrah and N. R. Abdelal, Improvement of the mode I interlaminar fracture toughness of carbon fiber composite reinforced with electrospun nylon nanofiber, *Composites, Part B*, 2019, **165**, 379–385.

84 H. J. Kim and J. H. Song, Improvement in the mechanical properties of carbon and aramid composites by fiber surface modification using polydopamine, *Composites, Part B*, 2019, **160**, 31–36.

85 S. Li, X. Li, M. Shao, J. Yang, Q. Wang, T. Wang and X. Zhang, Regulating interfacial compatibility with amino silane and bio-inspired polydopamine for high-performance epoxy composites, *Tribol. Int.*, 2019, **140**, 105861.

86 X. Chen, H. Xu, D. Liu, C. Yan and Y. Zhu, A novel and facile fabrication of polyphosphazene nanotube/carbon fiber multi-scale hybrid reinforcement and its enhancing effect on the interfacial properties of epoxy composites, *Compos. Sci. Technol.*, 2019, **169**, 34–44.

87 J. Dong, C. Jia, M. Wang, X. Fang, H. Wei, H. Xie, T. Zhang, J. He, Z. Jiang and Y. Huang, Improved mechanical properties of carbon fiber-reinforced epoxy composites by growing carbon black on carbon fiber surface, *Compos. Sci. Technol.*, 2017, **149**, 75–80.

88 M. D. R. Batista and L. T. Drzal, Carbon fiber/epoxy matrix composite interphases modified with cellulose nanocrystals, *Compos. Sci. Technol.*, 2018, **164**, 274–281.

89 W. Zhang, X. Deng, G. Sui and X. Yang, Improving interfacial and mechanical properties of carbon nanotube-sized carbon fiber/epoxy composites, *Carbon*, 2019, **145**, 629–639.

90 Z. Yao, C. Wang, J. Qin, S. Su, Y. Wang, Q. Wang, M. Yu and H. Wei, Interfacial improvement of carbon fiber/epoxy composites using one-step method for grafting carbon nanotubes on the fibers at ultra-low temperatures, *Carbon*, 2020, 133–142.

91 T. Li, M. Li, Y. Gu, S. Wang, Q. Li and Z. Zhang, Mechanical enhancement effect of the interlayer hybrid CNT film/carbon fiber/epoxy composite, *Compos. Sci. Technol.*, 2018, **166**, 176–182.

92 L. Chen, H. Jin, Z. Xu, J. Li, Q. Guo, M. Shan, C. Yang, Z. Wang, W. Mai and B. Cheng, Role of a gradient interface layer in interfacial enhancement of carbon fiber/epoxy hierarchical composites, *J. Mater. Sci.*, 2015, **50**(1), 112–121.

93 X. Zhang, X. Fan, C. Yan, H. Li, Y. Zhu, X. Li and L. Yu, Interfacial microstructure and properties of carbon fiber composites modified with graphene oxide, *ACS Appl. Mater. Interfaces*, 2012, **4**(3), 1543–1552.

94 J. Jiang, X. Yao, C. Xu, Y. Su, L. Zhou and C. Deng, Influence of electrochemical oxidation of carbon fiber on the mechanical properties of carbon fiber/graphene oxide/epoxy composites, *Composites, Part A*, 2017, **95**, 248–256.

95 L. Ma, Y. Zhu, P. Feng, G. Song, Y. Huang, H. Liu, J. Zhang, J. Fan, H. Hou and Z. Guo, Reinforcing carbon fiber epoxy composites with triazine derivatives functionalized graphene oxide modified sizing agent, *Composites, Part B*, 2019, **176**, 107078.

96 F. Yan, L. Liu, M. Li, M. Zhang, L. Xiao and Y. Ao, Preparation of carbon nanotube/copper/carbon fiber hierarchical composites by electrophoretic deposition for enhanced thermal conductivity and interfacial properties, *J. Mater. Sci.*, 2018, **53**(11), 8108–8119.

97 C. Wang, M. Zhao, J. Li, J. Yu, S. Sun, S. Ge, X. Guo, F. Xie, B. Jiang and E. K. Wujcik, Silver nanoparticles/graphene oxide decorated carbon fiber synergistic reinforcement in epoxy-based composites, *Polym*, 2017, **131**, 263–271.

98 L. Ma, Y. Zhu, X. Li, C. Yang, P. Han and G. Song, The architecture of carbon fiber-TiO2 nanorods hybrid structure in supercritical water for reinforcing interfacial and impact properties of CF/epoxy composites, *Polym. Test.*, 2018, **66**, 213–220.

99 L. Ma, N. Li, G. Wu, G. Song, X. Li, P. Han, G. Wang and Y. Huang, Interfacial enhancement of carbon fiber composites by growing TiO_2 nanowires onto amine-based functionalized carbon fiber surface in supercritical water, *Appl. Surf. Sci.*, 2018, **433**, 560–567.

100 L. Xiong, F. Zhan, H. Liang, L. Chen and D. Lan, Chemical grafting of nano-TiO_2 onto carbon fiber *via* thiol–ene click chemistry and its effect on the interfacial and mechanical properties of carbon fiber/epoxy composites, *J. Mater. Sci.*, 2018, **53**(4), 2594–2603.

101 S. M. Fakhrhoseini, Q. Li, V. Unnikrishnan and M. Naebe, Nano-magnetite decorated carbon fibre for enhanced interfacial shear strength, *Carbon*, 2019, **148**, 361–369.

102 L. Guadagno, M. Raimondo, C. Naddeo, P. Longo and W. H. Binder, in *Self-healing Polymers: from Principles to Applications*, Wiley-VCH Books, Weinheim, 2013, pp. 401–412.

103 R. Das, C. Melchior and K. M. Karumbaiah, Self-healing composites for aerospace applications, in *Advanced Composite Materials for Aerospace Engineering*, Elsevier, 2016, pp. 333–364.

104 D. G. Bekas, K. Tsirka, D. Baltzis and A. S. Paipetis, Self-healing materials: A review of advances in materials, evaluation, characterization and monitoring techniques, *Composites, Part B*, 2016, **87**, 92–119.

105 D. Y. Wu, S. Meure and D. Solomon, Microencapsulation of isocyanates for self-healing polymers, *Prog. Polym. Sci.*, 2008, **33**, 479–522.

106 S. Ruan, S. Wei, W. Gong, Z. Li, J. Gu and C. Shen, Strengthening, toughening, and self-healing for carbon fiber/epoxy composites based on PPESK electrospun coaxial nanofibers, *J. Appl. Polym. Sci.*, 2021, **138**(12), 50063.

107 M. Kosarli, G. Foteinidis, K. Tsirka, D. G. Bekas and A. S. Paipetis, Concurrent recovery of mechanical and electrical properties in nanomodified capsule-based self-healing epoxies, *Polymer*, 2021, 123843.

108 E. N. Brown, S. R. White and N. R. Sottos, Microcapsule induced toughening in a self-healing polymer composite, *J. Mater. Sci.*, 2004, **39**(5), 1703–1710.

109 J. D. Rule, N. R. Sottos and S. R. White, Effect of microcapsule size on the performance of self-healing polymers, *Polymer*, 2007, **48**(12), 3520–3529.

110 Q. Li, N. H. Kim, D. Hui and J. H. Lee, Effects of dual component microcapsules of resin and curing agent on the self-healing efficiency of epoxy, *Composites, Part B*, 2013, **55**, 79–85.

111 M. R. Kessler, N. R. Sottos and S. R. White, Self-healing structural composite materials, *Composites, Part A*, 2003, **34**(8), 743–753.

112 K. Sanada, I. Yasuda and Y. Shindo, Transverse tensile strength of unidirectional fibre-reinforced polymers and self-healing of interfacial debonding, *Plast., Rubber Compos.*, 2006, **35**(2), 67–72.

113 K. S. Toohey, N. R. Sottos, J. A. Lewis, J. S. Moore and S. R. White, Self-healing materials with microvascular networks, *Nat. Mater.*, 2007, **6**(8), 581–585.

114 K. S. Toohey, C. J. Hansen, J. A. Lewis, S. R. White and N. R. Sottos, Delivery of two part self healing chemistry *via* microvascular networks, *Adv. Funct. Mater.*, 2009, **19**(9), 1399–1405.

115 C. J. Norris, G. J. Meadway, M. J. O'Sullivan, I. P. Bond and R. S. Trask, Self-healing fibre reinforced composites *via* a bioinspired vasculature, *Adv. Funct. Mater.*, 2011, **21**(19), 3624–3633.

116 G. Williams, R. Trask and I. Bond, A self-healing carbon fibre reinforced polymer for aerospace applications, *Composites, Part A*, 2007, **38**(6), 1525–1532.

117 G. J. Williams, I. P. Bond and R. S. Trask, Compression after impact assessment of self-healing CFRP, *Composites, Part A*, 2009, **40**(9), 1399–1406.

118 X. F. Wu, A. Rahman, Z. Zhou, D. D. Pelot, S. Sinha Ray, B. Chen, S. Payne and A. L. Yarin, Electrospinning core–shell nanofibers for interfacial toughening and self healing of carbon fiber/epoxy composites, *J. Appl. Polym. Sci.*, 2013, **129**(3), 1383–1393.

119 R. E. Neisiany, J. K. Y. Lee, S. N. Khorasani and S. Ramakrishna, Self healing and interfacially toughened carbon fibre-epoxy composites based on electrospun core shell nanofibres, *J. Appl. Polym. Sci.*, 2017, **134**(31), 44956.

120 Y. Zhu, X. J. Ye, M. Z. Rong and M. Q. Zhang, Self-healing glass fiber/epoxy composites with polypropylene tubes containing self-pressurized epoxy and mercaptan healing agents, *Compos. Sci. Technol.*, 2016, **135**, 146–152.

121 R. E. Neisiany, J. K. Y. Lee, S. N. Khorasani, R. Bagheri and S. Ramakrishna, Facile strategy toward fabrication of highly responsive self-healing carbon/epoxy composites *via* incorporation of healing agents encapsulated in poly(methylmethacrylate) nanofiber shell, *J. Ind. Eng. Chem.*, 2018, **59**, 456–466.

122 D. L. Boger and S. M. Weinreb, *Hetero Diels-Alder Methodology in Organic Synthesis*, Elsevier, 1987.

123 J. Sauer, Diels-alder reactions II: The Reaction Mechanism, *Angew. Chem., Int. Ed. Engl.*, 1967, **6**(1), 16–33.

124 X. Chen, F. Wudl, A. K. Mal, H. Shen and S. R. Nutt, New thermally remendable highly cross-linked polymeric materials, *Macro*, 2003, **36**(6), 1802–1807.

125 F. Ghezzo, D. R. Smith, T. N. Starr, T. Perram, A. F. Starr, T. K. Darlington, R. K. Baldwin and S. J. Oldenburg, Development and characterization of healable carbon

fiber composites with a reversibly cross linked polymer, *J. Compos. Mater.*, 2010, **44**(13), 1587–1603.

126 W. Zhang, J. Duchet and J.-F. Garard, Self-healable interfaces based on thermo-reversible Diels-Alder reactions in carbon fiber reinforced composites, *J. Colloid Interface Sci.*, 2014, **430**, 61–68.

127 W. Zhang, J. Duchet and J. F. Garard, Effect of epoxy matrix architecture on the self-healing ability of thermo-reversible interfaces based on Diels-Alder reactions: demonstration on a carbon fiber/epoxy microcomposite, *RSC Adv.*, 2016, **6**(115), 114235–114243.

128 V. Kostopoulos, A. Kotrotsos, S. Tsantzalis, P. Tsokanas, A. C. Christopoulos and T. Loutas, Toughening and healing of continuous fibre reinforced composites with bis-maleimide based pre-pregs, *Smart Mater. Struct.*, 2016, **25**(8), 084011.

129 S. D. Iacono, A. Martone and E. Amendola, Diels-Alder Chemistry to Develop Self-Healing Epoxy Resins and Composites Thereof, in *Paint and Coatings Industry*, IntechOpen, 2018.

130 V. Kostopoulos, A. Kotrotsos, A. Sousanis and G. Sotiriadis, Fatigue behaviour of open-hole carbon fibre/epoxy composites containing bis-maleimide based polymer blend interleaves as self-healing agent, *Compos. Sci. Technol.*, 2019, **171**, 86–93.

131 P. Banerjee, S. Kumar and S. Bose, Thermoreversible Bonds and Graphene Oxide Additives Enhance the Flexural and Interlaminar Shear Strength of Self-Healing Epoxy/Carbon Fiber Laminates, *ACS Appl. Nano Mater.*, 2021, 6821–6831.

132 S.-J. Park and J.-R. Lee, Bending fracture and acoustic emission studies on carbon-carbon composites: effect of sizing treatment on carbon fibres, *J. Mater. Sci.*, 1998, **33**(3), 647–651.

133 Z. Dai, F. Shi, B. Zhang, M. Li and Z. Zhang, Effect of sizing on carbon fiber surface properties and fibers/epoxy interfacial adhesion, *Appl. Surf. Sci.*, 2011, **257**(15), 6980–6985.

134 Y. Li, B. Jiang and Y. Huang, Constructing nanosheet-like MOF on the carbon fiber surfaces for improving the interfacial properties of carbo fiber/epoxy composites, *Appl. Surf. Sci.*, 2020, 145870.

135 W. Shen, R. Ma, A. Du, X. Cao, H. Hu, Z. Wu, X. Zhao, Y. Fan and X. Cao, Effect of carbon nanotubes and octa-aminopropyl polyhedral oligomeric silsesquioxane on the surface behaviors of carbon fibers and mechanical performance of composites, *Appl. Surf. Sci.*, 2018, **447**, 894–901.

136 B. Anasori, M. R. Lukatskaya and Y. Gogotsi, 2D metal carbides and nitrides (MXenes) for energy storage, *Nat. Rev. Mater.*, 2017, **2**(2), 1–17.

137 M. Naguib, V. N. Mochalin, M. W. Barsoum and Y. Gogotsi, 25th anniversary article: MXenes: a new family of two dimensional materials, *Adv. Mater.*, 2014, **26**(7), 992–1005.

138 L. Liu, G. Ying, C. Hu, K. Zhang, F. Ma, L. Su, C. Zhang and C. Wang, Functionalization with MXene (Ti_3C_2) enhances the wettability and shear strength of carbon fiber-epoxy composites, *ACS Appl. Nano Mater.*, 2019, **2**(9), 5553–5562.